A Comprehensive Preferential Load Shedding Technique

by

Rehana Nasreen

A Thesis submitted to the Department of the Electrical and Electronic Engineering of Bangladesh University of Engineering and Technology in partial fulfillment of the requirements for the degree of

Master of Science in Electrical and Electronic Engineering

Department of Electrical and Electronic Engineering

BANGLADESH UNIVERSITY OF ENGINEERING AND TECHNOLOGY

Dhaka 1000, Bangladesh

May 2012

The thesis titled **"A Comprehensive Preferential Load Shedding Technique"** submitted by Rehana Nasreen, Roll No. 100606101P, Session: December 2005, has been accepted as satisfactory in partial fulfillment of the requirement for the degree of **Master of Science in Electrical and Electronic Engineering** on May 16, 2012.

BOARD OF EXAMINERS

1. _____
   Dr. Abdul Hasib Chowdhury — Chairman (Supervisor)
   Associate Professor
   Department of Electrical and Electronic Engineering
   BUET, Dhaka 1000, Bangladesh

2. _____
   Dr. Md. Saifur Rahman — Member (Ex-officio)
   Professor and Head
   Department of Electrical and Electronic Engineering
   BUET, Dhaka 1000, Bangladesh

3. _____
   Dr. Md. Quamrul Ahsan — Member
   Professor
   Department of Electrical and Electronic Engineering
   BUET, Dhaka 1000, Bangladesh

4. _____
   Dr. Kazi Mujibur Rahman — Member
   Professor
   Department of Electrical and Electronic Engineering
   BUET, Dhaka 1000, Bangladesh

5. _____
   Dr. Md. Fayyaz Khan — Member (External)
   Professor and Head
   Department of Electrical and Electronic Engineering
   United International University, Dhaka, Bangladesh

Declaration

It is hereby declared that this thesis titled **"A Comprehensive Preferential Load Shedding Technique"** or any part of it has not been submitted elsewhere for the award of any degree or diploma.

Signature of the candidate

_____

Rehana Nasreen

Acknowledgement

First of all, the author is grateful to almighty ALLAH for overcoming all the difficulties and problems that she faced during this study and for bringing this thesis into reality. The author wants to show her sincere gratitude to all individuals, who provided support, advice and encouragement during her student life in all the institutions.

The author is delighted to express her heartiest gratitude and sincerest indebtedness to her teacher, Dr. Abdul Hasib Chowdhury, Associate Professor, Department of Electrical and Electronics Engineering, Bangladesh University of Engineering and Technology, Dhaka, who served as her thesis supervisor. He provided information, useful suggestion, criticism and encouragement that enabled the author to carry out this study.

The author is deeply grateful to Dr. Md. Quamrul Ahsan, Professor, EEE, BUET for his all time guidance and suggestions.

Last but not the least, the author wants to express her indebtedness to her parents, her sister, her husband and her son for their all time support and encouragement during the study.

ABSTRACT

Load shedding is an emergency control action designed to ensure system stability by curtailing system load to match generation supply. Load-shedding for preventing frequency degradation is an established practice all over the world. Typically load shedding protects against excessive frequency or voltage decline by attempting to balance real and reactive power supply and demand in the system. If a considerable amount of generation is lost, the only effective way of correcting the imbalance would be to quickly shed loads before frequency falls so low that the power system collapses. Utilities would only resort to load shedding as a final measure and this action has the advantage of disconnecting selected loads for a relatively short period, rather than interrupting all consumers for extended periods.

In a power system network, the response of a generator closer to the point of disturbance that creates the imbalance between the load and generation is faster than that of a generator located at a far distant location with respect to the disturbance. At the moment of any disturbance that creates the imbalance between the load and generation, imbalance between the system load and generation is distributed among the generators according to their electrical distance with the load change location. Study will be made to analyze and qualitatively determine the time response of system frequency for load changes at different locations.

As the load imbalance distribution changes with time, the imbalance is distributed according to the inertias of generators. Study will be made to analyze and qualitatively determine the effect of generator *H* constant on the system frequency with sudden change in load.

It is expected that initially the impact of load change will be shared immediately by the generators according to their synchronizing power coefficients with respect to the bus at which the load change occurs. Thus, the machines electrically close to the point of impact will pick up the greater share of the load change regardless of their size. After a while it is expected that the imbalance will be shared according to the generator H constant.

Furthermore, the size of the load to be shed in an emergency situation is also important to stabilize the power system network quickly. Considering the importance of load size in this respect, loads are also ranked based on their magnitude.

Based on the above analysis, a shedding-index will be determined for each load buses depending on the electrical proximity of the loads to generators, the generator inertia constant (*H)* and the size of the load. The shedding-index shall help to prepare a priority list for shedding loads in a power system to achieve faster frequency stability under a fault condition. The performance of the proposed technique will be verified on a test network.

Contents

LIST OF TABLES

LIST OF FIGURES

List of Abbreviations

ROCOF	Rate of Change of Frequency
SFR	System Frequency Response
UFLS	Under Frequency Load Shedding Scheme
ILS	Intelligent Load Shedding
TNB	Tenaga National Berhad
PMS	Power Management System
ANN	Artificial Neural Network
DILS	Distributed Interruptible Load Shedding

List of Principal Symbols

H	Machine Inertia Constant
D	Generator Damping
$\overline{Y_{ii}}$	Driving point admittance of node i
$\overline{Y_{ij}}$	Negative of the transfer admittance between nodes i and j
P_i	Power into the network at node i
$\overline{I}$	Current
$\overline{E}$	Voltage
$P_{L\Delta}$	Small Load change
P_i	Power into the node i
$P_{i\Delta}$	Output Power
P_{sik}	Synchronizing power coefficients of node i with respect to the bus k.
$\overline{\delta}$	Angle
$\overline{\omega}$	Angular velocity
x_i	State variables
u	Column vector
g	Vector of nonlinear functions relating state and input variables to output variables
Δx	State vector of dimension n
Δy	Output vector of dimension m
Δu	Input vector of dimension r
A	State or plant matrix of size nxn
B	Control or input matrix of size nxr

C Output matrix of size *mxn*

D Feedforwarded matrix which defines the proportion of input which appears directly in the output, size *mxr*

Φ $n \times 1$ vector

ϕ_i Eigenvector

Λ Diagonal matrix

P Participation matrix

Δx State vector

Δy Single output

E_B Infinite bus voltage

P_e Air gap power

T_e Air gap torque

T_a Accelerating torque in N.m

T_m Mechanical torque in N.m

T_e Electromagnetic torque in N.m

J Combined moment of inertia of generator and turbine kg.m²

ω_m Angular velocity of the rotor in rad/s

t Time, sec

$\Delta\omega_r$ Per unit speed deviation

ω_0 Base rotor electrical speed in radians/sec

K_S Synchronizing torque coefficient

T_s Settling time

λ Eigen value

ζ Damping ratio

ω_n Undamped natural frequency

x_2 Electrical distance

CHAPTER 1

INTRODUCTION

1.1 Introduction

Load shedding is the term used to describe the deliberate switching off of electrical supply to parts of the electricity network, and hence to the customers in those areas. It may be required when there is an imbalance between load and generation. When there is a shortfall in the generation, there is a need to reduce demand very quickly to an acceptable level, or risk the entire electricity network becoming unstable and shutting down completely. Load shedding is a core part of the emergency management of all electricity networks.

1.2 Load Shedding Schemes

Load shedding schemes are important and powerful tools in the present day power systems to maintain system stability [1]. Typically load shedding protects against excessive frequency decline which may lead to blackout by attempting to balance load and generation. The three main categories of load shedding schemes are: (i) traditional, (ii) semi-adaptive and (iii) adaptive [2].

The traditional load shedding is mostly used among the three schemes, because it is simple and does not require sophisticated relays. The traditional scheme sheds a certain amount of the load when the system frequency falls below a certain threshold [3]. If this load drop is sufficient, the frequency will stabilize or increase. If this first load shed is not sufficient, the frequency keeps on falling, but at a slower rate. When the falling frequency reaches a second threshold, a second block of load is shed. This process is continued until the overload is relieved or all the frequency relays have operated. The values of the thresholds and the relative amount of load to be shed are decided off-line, based on experience and simulations. Traditional load shedding scheme has mostly conservative settings because of the lack of information regarding the magnitude of the disturbance. Although this approach is effective in preventing inadvertent load shedding in response to small disturbances with relatively longer time delay and lower frequency threshold, it is not able to distinguish between the normal oscillations of the power system and large disturbances. Thus, this approach is prone to shedding fewer loads.

The semi-adaptive load shedding scheme uses the frequency decline rate as a measure of the generation shortage. This scheme measures the rate of change of frequency (*df/dt*) (ROCOF) when a certain frequency threshold is reached [4]. According to the value of ROCOF, a different amount of load is shed. That is, this scheme checks also the speed at which the threshold is exceeded: the higher the speed is, the more load is shed. Usually, the measure of the rate of change of frequency is evaluated only at the first frequency threshold, the subsequent ones being traditional. In this scheme the ROCOF thresholds and the size of load blocks to be shed at different thresholds are decided off-line, on the basis of simulation and experience. But the scheme adapts to the system disturbance as the actual amount of load blocks to be shed is decided by the ROCOF relay depending on the rate of frequency change.

Adaptive load shedding scheme uses the frequency derivative and is based on the system frequency response (SFR) model developed in [5]. A reduced order SFR model is used to obtain a relation between the initial value of ROCOF and the size of the disturbance that caused the frequency decline [6]. Accordingly, the amount of load to be shed and its location is determined in real time.

Sometimes, blackout can be prevented in real time through controlled disintegration of a system into a number of islands together with generation and/or load shedding. Splitting a grid system into a number of independent islands can be considered either as a last resort or as a primary measure depending upon the structure of the system. The basis for islanding is never unique but rather depends upon the utility in particular.

In reference [7-10] different load shedding schemes are described based on frequency thresholds, rate of change of frequency, frequency and voltage changes, magnitude of the disturbance, load frequency regulation factor or system islanding depending on rate of change of frequency or real time monitoring of active-power (Megawatt) flows. All of them fall under any of the three categories described above.

In [7] a self-healing strategy is proposed to deal with catastrophic events when power system vulnerability analysis indicates that the system is approaching an extreme emergency state. Here the system is adaptively divided into smaller islands with considerations for quick restoration. After islanding, a load shedding scheme based on the rate of frequency decline is applied. This load shedding scheme raises the stability performance of the system by shedding less load compared to the conventional load shedding scheme. Since the tripping

action does not require much calculations and the islanding information can be obtained offline, the speed in the real-time implementation mostly depend on the speed of communication devices and switching actions. In order to facilitate restoration, the islands are formed by minimizing the generation-load imbalance.

The way, a blackout can be prevented in real time through controlled segregation of a system into a number of viable islands together with generation and/or load shedding is described in [8]. The nature and location of any fault that warrants such islanding is ascertained in real time through monitoring the active-power (megawatt) flows at both ends of a number of pre-specified lines. An intersection line is tripped due to a fault if the megawatt flow changes between two successive sampling instants by more than a threshold percentage at both ends of the line or else it will remain intact. This results in splitting the system into two or more islands or none at all depending upon the severity and location of the fault.

In [9] a new load shedding scheme utilizing frequency and voltage changes to shed loads specifically in the most affected localities while regaining the load-generation balance for each incident is described. Here a new arrangement is proposed, using voltage, frequency and rate of frequency change, to actuate and direct load shedding in proximity of the lost generation.

In [10] a slow coherency based islanding strategy is developed for large disturbances. The analytical basis for an application of slow coherency theory to the design of an islanding scheme is provided which is employed as an important part of a corrective control strategy to deal with large disturbances. The results indicate that the slow coherency based grouping is almost insensitive to locations and severity of the initial faults. However, because of the loosely coherent generators and physical constraints the islands formed change slightly based on location and severity of the disturbance, and loading conditions. A detailed description of the procedure to form the islands after having determined the grouping of generators using slow coherency is presented. This includes the development of the procedure for grouping and the identification of the weakest link in the network based on the slow coherency grouping.

A defense system based on load shedding, which can assess power system vulnerability and perform self-healing, corrective, and preventive control actions, is proposed in [11]. To provide greater flexibility and intelligence, the defense system is designed with multi agent system technologies.

A new procedure for protecting electric power systems from dynamic instability and frequency collapse is presented in [12]. It consists of two main stages. In the first stage, the frequency and the rate of frequency change are estimated by the non recursive Newton-type algorithm of the generator swing equation. In the second algorithm stage, the magnitude of the disturbance is determined. From the estimated disturbance, the number of steps, frequencies, the time delays, and the amount of load to be disconnected from the network in every step is determined

In [13] the objectives and principles of under frequency load shedding (UFLS) are reviewed, and reported their application to a small island power system is reported.

In [16], it is reported that shedding loads near the lost generator is more effective. But no detailed work is presented.

In [17], a new load shedding technique based on magnitude and rate of change of frequency during abnormal condition is developed. In an extreme condition, the grid is disintegrated forming islands and individual islands are brought to stable condition. Sensitivity of system frequency to the change of loads at different locations and the size of loads are used to categorize load centers.

A technique of choosing the load shedding point based on the on-line measurement of loads and the derivative of active power with respect to frequency i.e. load frequency regulation factor, is described in [14]. Loads with smaller frequency regulation factors are shed earlier than those with larger frequency regulation factors.

Frequency behavior of generators is studied in [15]. After occurrence of a disturbance in the network the frequency behavior of a generator depends on different parameters of the generator and its location, which includes electrical distance to disturbance location, generator inertia constant (H), generator damping (D), governor gain. It is observed that generator damping has no significant effect on the initial frequency behavior of generator after a disturbance. Change in the governor gain has almost no effect on frequency behavior of that generator. Minimum frequency deviations belong to the generators that have larger inertia constant, greater electrical distance from disturbance location and less electrical distance from slack generator. Amount of overload, disturbing condition and overload values are calculated first and then values of load to be shed is determined.

In [18], it is described that immediately after the load change impact in a power system network, the machines share the impact immediately according to their electrical proximity to the point of impact and after a brief transient period the same machines share the same impact according to their inertia constants.

Paper [19] has introduced an intelligent, optimal, and fast load shedding technology referred to as ILS (Intelligent Load Shedding). ILS combines online data, equipment ratings, user-defined control logics, and a knowledgebase obtained from power system simulation studies, to continually update dynamic load shed tables. Simulation of case studies for two industrial electrical networks are performed to demonstrate the advantages of an intelligent load shedding system over conventional load shedding methods from the design and operation perspectives.

Paper [20] describes the application of under-frequency load shedding scheme with dynamic D-factors, i.e., load frequency and voltage dependent coefficients, of various dynamic load models to Taiwan power system. The load models adopted are 1) a single-motor dynamic model, 2) a two-motor (one small and one large) dynamic model, and 3) a composite (static and dynamic) model. First, the dynamic *D*-factor values of these load models are determined by the actual analytical approach employed in Taiwan power system. Then, a single-machine model representing a multi-machine power system is utilized for validating the proposed load shedding scheme with derived dynamic *D*-factor values.

Paper [21] reports a case study on Malaysia's TNB (Tenaga National Berhad) system. UFLS scheme used by TNB is reviewed, Then modification and improvement is suggested to reflect the current changes in the system making the scheme more up to date. Effect of having more stages to reduce over shedding and combination of different amount of load at each stage are discussed.

Reference [22] presents a new adaptive load-shedding scheme for the Kosovo power system that provides emergency protection against excess frequency decline, in cases when the system is disconnected from the regional transmission network. The proposed load-shedding scheme uses the local frequency rate information to adapt the load-shedding pattern to suit the size and location of the occurring disturbance. Power flow and dynamic analysis are made in order to check the influence of island mode of operation of the Kosovo power system and to ensure proper load shedding scheme.

The load-shedding application presented in the paper [23] involves a large petrochemical facility. The primary scheme uses a comprehensive power management system (PMS) that calculates predicted power deficits resulting from predetermined events (contingency based), using system inertia and governor response models for system generators. In addition to the primary contingency-based load shedding scheme, the application of under frequency relays acts as a secure secondary load-shedding scheme in the event that the primary scheme is unavailable.

In [24], several under frequency load shedding schemes are presented as special protection schemes to preserve the integrity of islands, formed following the outage of tie lines connecting two areas in a double area power system. Following the outage of tie lines in a double area power system the area with great import of power may face large deficiency of energy and consequently blackout may occur in the island. The paper proposes a special protection scheme, being capable of preserving the balance of generation and consumption in order to prevent major outage. Paper [25] describes an efficient computational methodology that can be used for calculating the appropriate strategy for load shedding protection in autonomous power systems. It extends an existing method that is based on the sequential Monte Carlo simulation approach for comparing alternative strategies by taking into account the amount of load to be shed and the respective risk for the system stability. Besides Monte Carlo simulation approach it incorporates properly designed artificial neural networks (ANN).

Normally, in contingencies, the difference between the power absorbed and the power produced is very low, often less than 1% of the latter. Therefore if all the loads participated in the load shedding program, the discomfort would be minimal, considering its usually short duration. According to this point of view, paper [26] presents a new approach to the load shedding program to guarantee the correct electrical system operation by increasing the number of participants. This new load control strategy is named Distributed Interruptible Load Shedding (DILS). The optimal load reduction request is found by minimizing the expected value of an appropriate cost function, thus taking the uncertainty about the power absorbed by each customer into account. Given a target load relief, the magnitude of the load reduction signal to be sent to customers participating in the DILS program is found with the help of a Gaussian approximation to the probability distribution of their interruptible load.

In [27], a simple low-order system frequency response model for the analysis of the power system dynamics, following a large load generation imbalance, is derived. The introduction of frequency of equivalent inertial center, f_c simplified the analysis of power system dynamics properties.

In all of these schemes the amount of load to be shed in each stage is described but the load shed amount for a particular bus has not been worked out. A comprehensive method of preferential shedding of loads has yet to be worked out.

1.3 Objectives

The overall objective of the work is to develop a technique for comprehensive preferential load shedding by indexing the load buses based on electrical proximity between load and generator, generator inertia constant (H) and size of the load for restoring the system frequency more quickly while removing fewer loads.

The proposed strategy of preferential load shedding will reduce the active power absorbed by the loads and make the system frequency restoration faster. The performance of the proposed technique will be verified on a test network.

1.4 Organization of the Thesis

This thesis contains five chapters including introductory chapter and conclusion chapter. Chapter One reviews different load shedding schemes currently in use. In Chapter Two mathematical analysis of load impact assessment is presented. In Chapter Three preferential load shedding methodology is described. In Chapter Four the proposed technique is implemented in a test system and simulation results are presented. In Chapter Five summery of the work and future scope of work are described.

CHAPTER 2

LOAD IMPACT ASSESSMENT

2.1 Introduction

In this Chapter a classical model of a multimachine system is considered. From this system a theory is presented for load impact assessment.

2.2 Impact Assessment Using Small Signal Analysis

The state of a system represents the minimum amount of system information at any instant in time t_0 that is necessary so that its future behavior can be determined without reference to the input before t_0. Any set of *n* linearly independent system variables may be used to describe the state of the system. These are referred to as the state variables; they form a minimal set of dynamic variables that, along with the inputs to the system, provide a complete description of the system behavior.

The behavior of a dynamic system, such as a power system, may be described by a set of *n* first order nonlinear differential equation of the following form:

$$\dot{x}_i = f_i(x_1, x_2, ..., x_n; u_1, u_2, ..., u_r; t) \quad i=1,2,...,n \tag{2.1}$$

Where *n* is the order of the system and *r* is the number of inputs. The equation (2.1) can also be written in the form by using vector-matrix notation:

$$\dot{x} = f(x, u, t) \tag{2.2}$$

Where

$$x = \begin{bmatrix} x_1 \\ x_2 \\ . \\ . \\ . \\ x_n \end{bmatrix} \qquad u = \begin{bmatrix} u_1 \\ u_2 \\ . \\ . \\ . \\ u_n \end{bmatrix} \qquad f = \begin{bmatrix} f_1 \\ f_2 \\ . \\ . \\ . \\ f_n \end{bmatrix}$$

The column vector x is referred to as the state vector, and its entries x_i as state variables. The column vector u is the vector of inputs to the system. These are the external signals that influence the performance of the system. Time is denoted by t, and the derivative of a state variable x with respect to time is denoted by $\dot{x}$. If the derivatives of the state variables are not explicit functions of time, the system is said to be autonomous.

In this case equation (2.2) simplifies to

$$\dot{x} = f(x,u) \tag{2.3}$$

The output variables which can be observed on the system may be expressed in terms of the state variables and the input variables in the following form:

$$y = g(x,u) \tag{2.4}$$

Where

$$y = \begin{bmatrix} y_1 \\ y_2 \\ . \\ . \\ . \\ y_m \end{bmatrix} \qquad g = \begin{bmatrix} g_1 \\ g_2 \\ . \\ . \\ . \\ g_m \end{bmatrix}$$

The column vector y is the vector of outputs, and g is a vector of nonlinear functions relating state and input variables to output variables.

If the functions f_i ($i=1,2,..,n$) in equation (2.3) are linear, then the system is linear. The equilibrium points are those points where all the derivatives $\dot{x}_1, \dot{x}_2, .\dot{x}_n$ are simultaneously zero; they define the points on the trajectory with zero velocity. A linear system has only one equilibrium state (if the system matrix is non-singular). For a nonlinear system there may be more than one equilibrium point.

The stability of a non linear system is entirely independent of the input, and the state of a stable system with zero input will always return to the origin of the state space, independent

of the finite initial state and the stability of a nonlinear system depends on the type and magnitude of input, and the initial state.

To linearize the equation (2.3), let x_0 be the initial state vector and u_0 the input vector corresponding to the equilibrium point about which the small signal performance is to be investigated. Since x_0 and u_0 satisfy the equation (2.3) we have

$$\dot{x}_0 = f(x_0, u_0) = 0 \tag{2.5}$$

The system is perturbed the system from the above state, by letting

$$x = x_0 + \Delta x$$

$$u = u_0 + \Delta u$$

where the prefix Δ denotes a small deviation, the new state must satisfy the equation (2.3). Hence,

$$\dot{x} = \dot{x}_0 + \Delta \dot{x} = f[(x_0 + \Delta x), (u_0 + \Delta u)] \tag{2.6}$$

As the perturbations are assumed to be small, the nonlinear functions *f(x,u)* can be expressed in terms of Taylor's series expansion. With terms involving second and third order powers of Δ*x* and Δ*u* neglected, we can write

$$\begin{aligned} x_i &= x_{i0} + \Delta x_i \\ &= f_i[(x_0 + \Delta x), (u_0 + \Delta u)] \\ &= f_i(x_0, u_0) + \frac{\partial f_i}{\partial x_1}\Delta x_1 + \ldots + \frac{\partial f_i}{\partial x_n}\Delta u_1 + \ldots + \frac{\partial f_i}{\partial u_r}\Delta u_r \end{aligned}$$

Since $\dot{x}_{i0} = f_i(x_0, u_0)$, we obtain

$$\Delta \dot{x}_i = \frac{\partial f_i}{\partial x_1}\Delta x_1 + \ldots + \frac{\partial f_i}{\partial x_n}\Delta x_n + \frac{\partial f_i}{\partial u_1}\Delta u_1 + \ldots + \frac{\partial f_i}{\partial u_r}\Delta u_r \qquad i=1,2,\ldots,n$$

In a like manner from equation (2.4) we have

$$\Delta y_j = \frac{\partial g_j}{\partial x_1}\Delta x_1 + ... + \frac{\partial g_j}{\partial x_n}\Delta x_n + \frac{\partial g_j}{\partial u_1}\Delta u_1 + ... + \frac{\partial g_j}{\partial u_r}\Delta u_r \qquad j=1,2,...,m$$

Therefore the linearized forms of equation (2.3) and (2.4) are

$$\Delta \dot{x} = A\Delta x + B\Delta u \tag{2.7}$$

and

$$\Delta y = C\Delta x + D\Delta u \tag{2.8}$$

Where

$$A=\begin{bmatrix} \frac{\partial f_1}{\partial x_1} & \cdots & \frac{\partial f_1}{\partial x_n} \\ \cdots & \cdots & \cdots \\ \frac{\partial f_n}{\partial x_1} & \cdots & \frac{\partial f_n}{\partial x_n} \end{bmatrix} \tag{2.9}$$

$$B=\begin{bmatrix} \frac{\partial f_1}{\partial u_1} & \cdots & \frac{\partial f_1}{\partial u_r} \\ \cdots & \cdots & \cdots \\ \frac{\partial f_n}{\partial u_1} & \cdots & \frac{\partial f_n}{\partial u_r} \end{bmatrix} \tag{2.10}$$

$$C=\begin{bmatrix} \frac{\partial g_1}{\partial x_1} & \cdots & \frac{\partial g_1}{\partial x_n} \\ \cdots & \cdots & \cdots \\ \frac{\partial g_m}{\partial x_1} & \cdots & \frac{\partial g_m}{\partial x_n} \end{bmatrix} \tag{2.11}$$

$$D=\begin{bmatrix} \frac{\partial g_1}{\partial u_1} & \cdots & \frac{\partial g_1}{\partial u_r} \\ \cdots & \cdots & \cdots \\ \frac{\partial g_m}{\partial u_1} & \cdots & \frac{\partial g_m}{\partial u_r} \end{bmatrix} \tag{2.12}$$

In the equations (2.7) and (2.8)

Δx = State vector of dimension n

Δy = Output vector of dimension *m*

Δu = Input vector of dimension *r*

A = State or plant matrix of size *nxn*

B = Control or input matrix of size *nxr*

C = Output matrix of size *mxn*

D = Feed-forward matrix which defines the proportion of input which appears directly in the output, size *mxr*

The eigen values of a matrix are given by the values of the scalar parameters λ for which there exist non-trivial solutions (other than $\phi=0$) to the equation

$$A\phi=\lambda\phi \tag{2.13}$$

A is an $n \times n$ matrix

Φ is an $n \times 1$ vector

To find the eigenvalues the equation (2.13) can be written as

$$(A-\lambda I)\phi=0 \tag{2.14}$$

For an non-trivial solution

$$det(A-\lambda I)=0 \tag{2.15}$$

Expansion of the determinant gives the characteristic equation, the *n* solutions of $\lambda=\lambda_1, \lambda_2, ..., \lambda_n$ are eigenvalues of *A*.

For any eigenvalue λ_i the n-column vector ϕ_i which satisfies the equation (2.13) is called right eigenvector of *A* associated with the eigenvalue λ_i.

$$A\phi_i = \lambda_i \phi_i \qquad i=1,2,....,n \tag{2.16}$$

The eigenvector ϕ_i has the form

$$\phi_i = \begin{bmatrix} \phi_{1i} \\ \phi_{2i} \\ . \\ . \\ . \\ \phi_{ni} \end{bmatrix}$$

The equation (2.14) is homogenous, $k\phi_i$ (where k is a scalar) is also a solution. Thus the eigenvectors are determined only to within a scalar multiplier.

Similarly, the n-row vector ψ_i which satisfies

$$\psi_i A = \lambda_i \psi_i \quad i=1,2,...,n \tag{2.17}$$

ψ_i is called the left eigenvector associated with the eigenvalue λ_i.

The left and right eigen vectors corresponding to the different eigenvalues are orthogonal. In other words if λ_i is equal to λ_j.

$$\psi_j \phi_i = 0 \tag{2.18}$$

However in the case of eigenvectors corresponding to the same eigenvalue

$$\psi_i \phi_i = C_i \tag{2.19}$$

where C_i is a non zero constant.

As the eigenvectors are determined only to within a scalar multiplier, it is common practice to normalize these vectors so that

$$\psi_I \phi_I = 1 \tag{2.20}$$

In order to express the eigen properties of A succinctly, the following matrices are introduced.

$$\phi = [\phi_1 \quad \phi_2 \quad .... \quad \phi_n] \tag{2.21}$$

$$\psi = [\psi_1^T \quad \psi_2^T \quad ... \quad \psi_n^T]^T \tag{2.22}$$

Λ = Diagonal matrix, with the eigenvalues $\lambda_1, \lambda_2, ..., \lambda_n$ as diagonal elements.

Each of the above matrices are $n \times n$

Equations (2.16) and (2.20) are expanded as follows.

$$A\phi = \phi\Lambda \tag{2.23}$$

$$\Psi\phi = I$$

、 $$\psi = \phi^{-1} \tag{2.24}$$

It follows from the equation (2.23)

$$\phi^{-1} A \phi = \Lambda \tag{2.25}$$

Referring to the state equation (2.8) the free motion (with zero input) is given by

$$\Delta \dot{x} = A\Delta x \tag{2.26}$$

In order to eliminate the cross coupling between the state variables, a new state vector z related to the original state vector Δx by the transformation is defined

$$\Delta x = \phi z \tag{2.27}$$

Where ϕ is the modal matrix of A defined by equation (2.21).

By substituting the above expression of equation (2.27) in the equation (2.26) we find

$$\phi \dot{z} = A\, \phi z \tag{2.28}$$

The new state equation can be written as

$$\dot{z} = \phi^{-1} A \phi z \tag{2.29}$$

In view of equation (2.25) the equation (2.29) becomes

$$\dot{z}=\Lambda z \tag{2.30}$$

The important difference between equations (2.30) and (2.26) is that Λ is a diagonal matrix whereas A, in general, is non-diagonal.

The response in terms of original state vector of the equation (2.27) is given by

$$\Delta x(t)=\phi z(t)$$

$$=\begin{bmatrix}\phi_1 & \phi_2 & \dots & \phi_n\end{bmatrix}\begin{bmatrix} z_1(t) \\ z_2(t) \\ . \\ . \\ . \\ z_n(t)\end{bmatrix} \tag{2.31}$$

In time response we can write the equation (2.31) in the below format

$$\Delta x(t)=\sum_{i=1}^{n}\phi_i z_i(0)e^{\lambda_i t} \tag{2.32}$$

From equation (2.27), we have

$$z(t)=\phi^{-1}\Delta x(t) = \psi \Delta x(t) \tag{2.33}$$

This implies that

$$z_i(t) = \psi_i \Delta x(t) \tag{2.34}$$

With $t=0$, it follows that

$$z_i(0) = \psi_i \Delta x(0) \tag{2.35}$$

By using c_i to denote the scalar product $\psi_i \Delta x(0)$, equation (2.32) can be written as

$$\Delta x(t)=\sum_{i=1}^{n} \phi_i c_i e^{\lambda_i t} \tag{2.36}$$

In other words the time response of i^{th} state variable can be written as

$$\Delta x_i(t) = \phi_{i1} c_1 e^{\lambda_1 t} + \phi_{i2} c_2 e^{\lambda_2 t} + \ldots + \phi_{in} c_n e^{\lambda_n t} \tag{2.37}$$

The above equation (2.37) gives the expression for the free motion time response of the system in terms of the eigen values and left and right eigenvectors.

The scalar product $c_i = \psi_i \Delta x(0)$ represents the magnitude of the excitation of the i^{th} mode resulting from the initial conditions.

One problem in using right and left eigenvectors individually for identifying the relationship between the states and the modes is that the elements of the eigenvectors are dependent on units and scaling associated with state variables. As a solution to this problem, a matrix called participation matrix (P), which combines the right and left eigenvectors. It is a measure of association between the state variables and the modes.

$$P=\begin{bmatrix} p_1 & p_2 & \ldots & p_n \end{bmatrix} \tag{2.38}$$

with

$$P_i = \begin{bmatrix} p_{1i} \\ p_{2i} \\ . \\ . \\ . \\ p_{ni} \end{bmatrix} = \begin{bmatrix} \phi_{1i}\psi_{i1} \\ \phi_{2i}\psi_{i2} \\ . \\ . \\ . \\ \phi_{ni}\psi_{in} \end{bmatrix} \tag{2.39}$$

where

ϕk_i = The element on the k_{th} row and ith column of the modal matrix ϕ

= k_{th} entry of the right eigenvector ϕ_i

ψ_{ik} = The element on the ith row and kth column of the modal matrix ψ

= k_{th} entry of the left eigen vector ψ_i

$p_{ki} = \phi_{ki}\psi_{ik}$ is termed as participation factor. It is a measure of the relative participation of the k_{th} state variable in the i_{th} mode, and vice versa.

For small signal stability analysis of power systems the transfer function between the variables *y* and *u* can be written as

$$\Delta \dot{x} = A\Delta x + b\Delta u \tag{2.40}$$

$$\Delta y = c\Delta x \tag{2.41}$$

Where

A = State matrix

Δx = State vector

Δu = Single input

Δy = Single output

c = Row vector

b = Column vector

2.3 Generator representation

The classical model representation of a generator collected to a large system is shown in Fig-2.1. Here all the resistances are neglected.

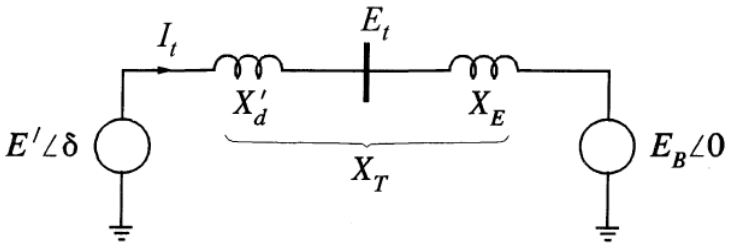

Fig-2.1: Classical model representation of a generator collected to a large system for measuring small signal performance

In Fig-2.1

$$X_T = X_d^{'} + X_E$$

E' is the voltage behind $X_d^{'}$. Its magnitude is assumed to remain constant at the pre disturbance value and δ is the angle by which E' leads the infinite bus voltage E_B. As the rotor oscillates during a disturbance, δ changes.

$$\widetilde{E}' = \widetilde{E}_{t0} + jX'_d\widetilde{I}_{t0}$$

With E' as reference phasor,

$$S' = P + jQ' = \widetilde{E}'\widetilde{I}* = \frac{E'E_B \sin\delta}{X_T} + j\frac{E'(E' - E_B\cos\delta)}{X_T} \tag{2.42}$$

With stator resistance neglected, the air-gap power (P_e) is equal to the terminal power (P). In per unit the air gap torque is equal to the air gap power. Hence

$$T_e = P = \frac{E'E_B}{X_T}\sin\delta \tag{2.43}$$

Linearizing about an initial operating condition represented by $\delta = \delta_0$ yields

$$\Delta T_e = \frac{\partial T_e}{\partial\delta}\Delta\delta = \frac{E'E_B}{X_T}\cos\delta_0(\Delta\delta) \tag{2.44}$$

Now from swing equation

$$J\frac{d\omega_m}{dt} = T_a = T_m - T_e \tag{2.45}$$

Where

T_a = Accelerating torque in N.m

T_m = Mechanical torque in N.m

T_e = Electromagnetic torque in N.m

J = Combined moment of inertia of generator and turbine kg.m²

ω_m = Angular velocity of the rotor in rad/s

t = Time, sec

The inertia constant, H in watt-sec at rated speed/VA base

$$H = \frac{1}{2}\frac{J\omega^2{}_{0m}}{VA_{base}} \tag{2.46}$$

Where

ω_{0m} = Rated angular velocity in mechanical radians/sec

Now substituting equation (2.46) in equation (2.45)

$$\frac{2H}{\omega^2{}_{0m}} VA_{base}\frac{d\omega_m}{dt} = T_m - T_e$$

The equation of motion in per unit form is

$$2H\frac{d\overline{\omega_r}}{dt} = \overline{T_m} - \overline{T_e} \tag{2.47}$$

As

$$T_{base} = \frac{VA_{base}}{\omega_{0m}}$$

In equation (2.47)

$$\overline{\omega_r} = \frac{\omega_m}{\omega_{0m}} = \frac{\omega_r / p_f}{\omega_0 / p_f} = \frac{\omega_r}{\omega_0}$$

Where

ω_r = Angular velocity of rotor in electrical rad/s

ω_0 = Rated value of angular velocity

p_f = Number of field poles

If δ is the angular position of the rotor in electrical radians with respect to a synchronously rotating reference and δ_0 is its value at *t=0*

$$\delta = \omega_r t - \omega_0 t + \delta_0 \tag{2.48}$$

Taking the time derivative we have

$$\frac{d\delta}{dt} = \omega_r - \omega_0 = \Delta\omega_r \tag{2.49}$$

and

$$\frac{d^2\delta}{dt^2} = \frac{d\omega_r}{dt} = \frac{d(\Delta\omega_r)}{dt} = \omega_0 \frac{d\overline{\omega_r}}{dt} = \omega_0 \frac{d(\Delta\overline{\omega_r})}{dt} \tag{2.50}$$

Substituting for $d\overline{\omega_r}/dt$ given by the above equation in equation (2.47) we get

$$\frac{2H}{\omega_0}\frac{d^2\delta}{dt^2} = \overline{T_m} - \overline{T_e} \tag{2.51}$$

It is often desirable to include a component of damping torque, not accounted for in the calculation of T_e, separately. This is accomplished by adding a term proportional to speed deviation in equation (2.51) as follows:

$$\frac{2H}{\omega_0}\frac{d^2\delta}{dt^2} = \overline{T_m} - \overline{T_e} - K_D\Delta\overline{\omega_r} \tag{2.52}$$

Equation (2.52) represents the equation of motion of a synchronous machine. It is commonly referred to as the swing equation because it represents swings in rotor angle δ during disturbances.

In equation (2.49)

$$\Delta\overline{\omega_r} = \frac{\Delta\omega_r}{\omega_0} = \frac{1}{\omega_0}\frac{d\delta}{dt} \tag{2.53}$$

From equations (2.52) and (2.53) we can write that

$$p\Delta\omega_r = \frac{1}{2H}(T_m - T_e - K_D\Delta\omega_r) \tag{2.54}$$

$$p\delta = \omega_0\Delta\omega_r \tag{2.55}$$

Where

$\Delta\omega_r$ =The per unit speed deviation

ω_0 =Base rotor electrical speed in radians/sec

p=Differential operator *d/dt* with time *t* in seconds

Linearizing equation (2.54) and substituting for ΔT_e given by equation (2.44) we can obtain

$$p\Delta\omega_r = \frac{1}{2H}[\Delta T_m - K_S\Delta\delta - K_D\Delta\omega_r] \tag{2.56}$$

Here K_S is the synchronizing torque coefficient given by

$$K_S = \left(\frac{E'E_B}{X_T} \right) \cos\delta_0 \tag{2.57}$$

Again we know

$$\lambda = -\zeta\omega_n \pm \omega_n \sqrt{(1-\zeta^2)}$$

where

λ =eigen value

ζ =damping ratio

ω_n =Undamped natural frequency

$$\omega_n = \sqrt{\frac{K_s \omega_0}{2H}}$$

so

$$K_s = \frac{2H\omega_n^2}{\omega_0} \tag{2.58}$$

and

$$\zeta = \frac{K_D}{2\sqrt{2K_s H\omega_0}}$$

so

$$K_s = \frac{K_D^2}{8H\omega_0\zeta^2} \tag{2.59}$$

Linearizing equation (2.38) we have

$$p\Delta\delta = \omega_0 \Delta\omega_r \tag{2.60}$$

Now writing the equations (2.56) and (2.60) in the vector-matrix form, we obtain

$$\frac{d}{dt}\begin{bmatrix}\Delta\omega_r\\ \Delta\delta\end{bmatrix}=\begin{bmatrix}-\frac{K_D}{2H} & -\frac{K_S}{2H}\\ \omega_0 & 0\end{bmatrix}\begin{bmatrix}\Delta\omega_r\\ \Delta\delta\end{bmatrix}+\begin{bmatrix}\frac{1}{2H}\\ 0\end{bmatrix}\Delta T_m \tag{2.61}$$

This is of the form $\dot{x} = Ax + bu$. The elements of the state matrix A are seen to be dependent on the system parameters K_D,H, X_T, and the initial operating condition represented by the values of E' and δ_0.

The time response of speed deviation is

$$\begin{bmatrix}\Delta\omega_r(t)\\ \Delta\delta(t)\end{bmatrix}=\begin{bmatrix}\phi_{11} & \phi_{12} & . & \phi_{1n}\\ \phi_{21} & \phi_{22} & . & \phi_{2n}\\ . & . & . & .\\ \phi_{n1} & \phi_{n2} & . & \phi_{nn}\end{bmatrix}\begin{bmatrix}c_1e^{\lambda_1 t}\\ c_2e^{\lambda_2 t}\\ .\\ c_ne^{\lambda_n t}\end{bmatrix} \tag{2.62}$$

Where

$$\begin{bmatrix}c_1\\ c_2\\ .\\ c_n\end{bmatrix}=\begin{bmatrix}\psi_{11} & \psi_{12} & . & \psi_{1n}\\ \psi_{21} & \psi_{22} & . & \psi_{2n}\\ . & . & . & .\\ \psi_{n1} & \psi_{n2} & . & \psi_{nn}\end{bmatrix}\begin{bmatrix}\Delta\omega_r(0)\\ \Delta\delta(0)\end{bmatrix}$$

2.4 Load impact on generators

Considering a classical model of a multimachine system, the following assumptions are made

1. The load has a negligible reactive component
2. The Mechanical power input is constant
3. Damping or asynchronous power is negligible
4. Constant voltage behind transient reactance model for the synchronous machines is valid
5. The mechanical rotor angle for a machine coincides with the angle of the voltage behind the transient reactance
6. Loads are represented by passive impedances

The electrical network obtained for an *n* machine system is shown in Fig-2.2 Node *0* is the reference node and nodes *1,2,..,n* are the internal machine buses or the buses to which the voltages behind transient reactances are applied.

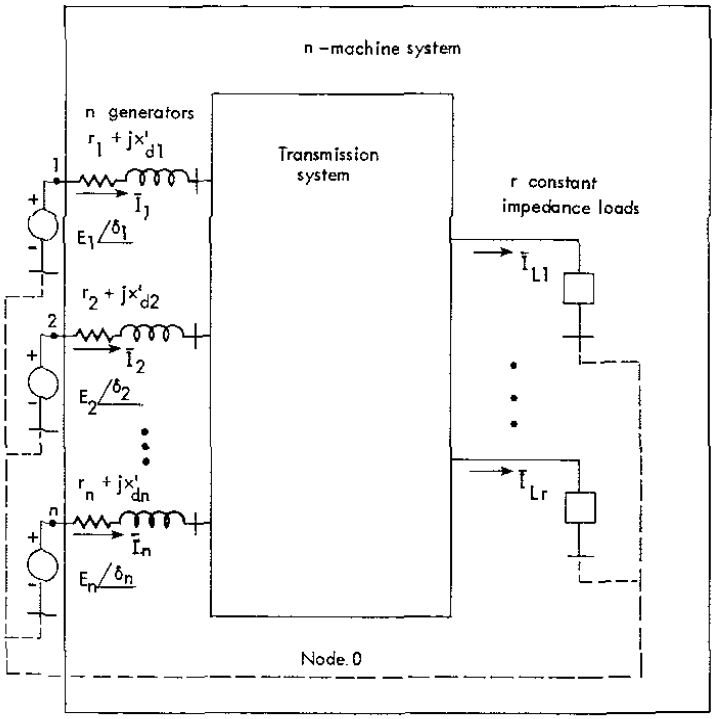

Fig-2.2: Representation of a multi machine system (Classical model)

Looking into the network from the terminals of the generators, it can be said from Fig-2.2

$$\bar{I} = \bar{Y}\,\bar{E}$$

Where $\bar{Y}$ has the diagonal elements $\overline{Y_{ii}}$ and the off diagonal elements $\overline{Y_{ij}}$

By definition

$$\overline{Y_{ii}} = Y_{ii}\angle\theta_{ii} = \text{Driving point admittance of node } i$$

$$= G_{ii} + \mathrm{j}\, B_{ii}$$

$\overline{Y_{ij}} = Y_{ij} \angle\theta_{ij}$ = Negative of the transfer admittance between nodes *i* and *j*

$= G_{ij} + \mathrm{j}\, B_{ij}$

The power into the network at node *i*, which is the electrical power output of machine *i*, is given by

$$P_i = \mathrm{Re}\ \overline{E_i}\ \overline{I_i}^{*}$$

$$P_{ei} = E_i^2 G_{ii} + \sum_{\substack{j=1 \\ j\neq i}}^{n} E_i E_j Y_{ij} \cos(\theta_{ij} - \delta_i + \delta_{j)} \qquad i=1,2,\ldots\ldots,n$$

$$= E_i^2 G_{ii} + \sum_{\substack{j=1 \\ j\neq i}}^{n} E_i E_j [B_{ij} \sin(\delta_i - \delta_j) + G_{ij} \cos(\delta_i - \delta_j)] \qquad i=1,2,\ldots\ldots,n$$

$$P_{ei} = E_i^2 G_{ii} + \sum_{\substack{j=1 \\ j\neq i}}^{n} E_i E_j [B_{ij} \sin\delta_{ij} + G_{ij} \cos\delta_{ij}] \qquad i=1,2,\ldots\ldots,n \qquad (2.63)$$

2.4.1 Linearization

The equation for injected power (2.63) is nonlinear because of the transcendental funcions. Since we are concerned only with a small impact $P_{L\Delta}$, these equations may be linearized to find

$$P_i = P_{i0} + P_{i\Delta}$$

And determine only the change variable, $P_{i\Delta}$.

Using the incremental model so that $\delta_{ij} = \delta_{ij0} + \delta_{ij\Delta}$

$$\sin\delta_{ij} = \sin\delta_{ij0}\cos\delta_{ij\Delta} + \cos\delta_{ij0}\sin\delta_{ij\Delta} \cong \sin\delta_{ij0} + \delta_{ij\Delta}\cos\delta_{ij0}$$

and

$$\cos\delta_{ij} \cong \cos\delta_{ij0} - \delta_{ij\Delta}\sin\delta_{ij0}$$

Finally $P_{ei\Delta} = \sum_{\substack{j=1 \\ j\neq i}}^{n} E_i E_j (B_{ij}\cos\delta_{ij0} - G_{ij}\sin\delta_{ij0})\delta_{ij\Delta}$ (2.64)

For a given network condition $\sin\delta_{ij0}$ and $\cos\delta_{ij0}$ are known and the term in parentheses in (2.64) is a constant.

So we can write,

$$P_{ei\Delta} = \sum_{\substack{j=1 \\ j\neq i}}^{n} P_{sij}\delta_{ij\Delta} \tag{2.65}$$

where, $P_{sij} \overset{\Delta}{=} \frac{\partial P_{ij}}{\partial \delta_{ij}}]_{\delta_{ij0}} = E_i E_j (B_{ij}\cos\delta_{ij0} - G_{ij}\sin\delta_{ij0})$

P_{sij} is the change in the electrical power of machine *i* due to a change in the angle between machine *i* and j with all other angles held constant. Its units are W/rad or pu power/rad. It is synchronizing power coefficient between nodes *i* and *j*.

For analyzing the effect of sudden application of a small load $P_{L\Delta}$ at some point in to the network, it is assumed that the load has a negligible reactive component to simplify the model. Since the sudden change in load $P_{L\Delta}$ creates an unbalance between generation and load, an oscillatory transient result before the system settles to a new steady state condition.

The phenomena may be mathematically formulated using the network configuration of Fig-2.3.

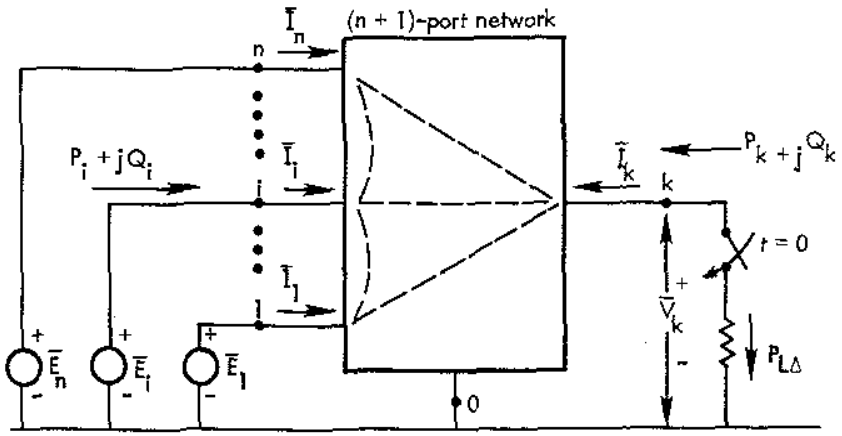

Fig-2.3: Circuit for measuring the effect of sudden application of a small load $P_{L\Delta}$ at some point *k* in the network

From the circuit in Fig 2.3, the power into the node *i* can be obtained from equation (2.63) by adding node *k*, where the load impact $P_{L\Delta}$ is applied.

$$P_i = E_i G_{ii} + \sum_{\substack{j=1 \\ j \neq ik}}^{n} E_i E_j (B_{ij} \sin\delta_{ij} + G_{ij} \cos\delta_{ij}) + E_i V_k (B_{ik} \sin\delta_{ik} + G_{ik} \cos\delta_{ik})$$

For the case of nearly zero conductance (as the network has a very large *X/R* ratio)

$$P_i \cong \sum E_i E_j B_{ij} \sin\delta_{ij} + E_i V_k B_{ik} \sin\delta_{ik}$$

The Power into the node *k*

$$P_k = \sum_{\substack{j=1 \\ j \neq k}}^{n} V_k E_j B_{kj} \sin\delta_{kj}$$

Assuming the network response to be fast the immediate effect of the application of $P_{L\Delta}$ is that the angle of bus *k* is changed while the magnitude of its voltage V_k is unchanged or $V_k \angle \delta_{k0}$ becomes $V_k \angle (\delta_{k0} + \delta_{k\Delta})$. The internal angles of machine nodes $\delta_1, \delta_2, \ldots, \delta_n$ do not change instantly because of the rotor inertia.

From (2.65) we can write that

$$P_{k\Delta} = \sum_{j=1}^{n} P_{skj}\delta_{kj\Delta} \tag{2.66}$$

The equation (2.66) is valid for any time *t* following the application of the impact.

2.4.2 Behavior for the special case $t = 0^+$

Let us now consider the case at $t=0^+$ where it can be determined exactly how much of the impact, $P_{L\Delta}$ is supplied by each generator $P_{i\Delta}$. *i=1,2,….n.*

At the instant $t=0^+$ we know that $\delta_{i\delta}=0$ for all generators because of rotor inertias. Here the change in voltage phase angle between buses may be written as

$$\delta_{ij\Delta} = 0$$

$$\delta_{ik\Delta} = \delta_{i\Delta} - \delta_{k\Delta} = -\delta_{k\Delta}(0^+)$$

$$\delta_{kj\Delta} = \delta_{k\Delta} - \delta_{j\Delta} = \delta_{k\Delta}(0^+)$$

So (2.64) becomes

$$P_{i\Delta}(0^+) = -P_{sik}\delta_{k\Delta}(0^+) \tag{2.67}$$

$$P_{k\Delta}(0^+) = \sum_{j=1}^{n} P_{skj}\delta_{k\Delta}(0^+) \tag{2.68}$$

Comparing the equations (2.67) and (2.68) at $t=0^+$, at node *k*

$$P_{k\Delta}(0^+) = -\sum_{i=1}^{n} P_{i\Delta}(0^+) \tag{2.69}$$

This is to be expected since a nearly reactive network is considered. It is also found that at node *i*, $P_{i\Delta} \propto B_{ik}\cos\delta_{ik0}$ i.e. $P_{i\Delta}$ depends upon $B_{ik}\cos\delta_{ik0}$. In other words, the higher the transfer susceptance B_{ik} and the lower initial angle δ_{ik0}, the greater the share of the impact picked up by the machine *i*.

As $P_{k\Delta} = -P_{L\Delta}$, the equations can be written in terms of the load impact as

$$P_{L\Delta}(0^+) = -\sum_{i=1}^{n} P_{ski}\delta_{k\Delta}(0^+) = \sum_{i=1}^{n} P_{i\Delta}(0^+) \tag{2.70}$$

So from equations (2.69) and (2.70) we can write that

$$\delta_{k\Delta}(0^+) = -\frac{P_{L\Delta}(0^+)}{\sum_{i=1}^{n} P_{sik}} \tag{2.71}$$

$$P_{i\Delta}(0^+) = \left(\frac{P_{sik}}{\sum_{j=1}^{n} P_{sjk}} \right) P_{L\Delta}(0^+) \qquad i=1,2,...,n \tag{2.72}$$

The equations (2.69) and (2.72) indicate that the load impact $P_{L\Delta}$ at a network bus k is immediately shared by the synchronous generators according to their synchronizing power coefficients with respect to the bus k.

Thus the machine electrically close to the point of impact will pick up the greater share of the load regardless of their size.

Let the deceleration of machine i due to sudden increase in its output power be $P_{i\Delta}$. Then the incremental differential equation governing the motion of machine i is

$$\frac{2H_i}{\omega_R}\frac{d\omega_{i\Delta}}{dt} + P_{i\Delta}(t) = 0 \qquad i=1,2,...,n \tag{2.73}$$

Using the equation (2.72)

$$\frac{2H_i}{\omega_R}\frac{d\omega_{i\Delta}}{dt} + \left(\frac{P_{sik}}{\sum_{j=1}^{n} P_{sjk}} \right) P_{L\Delta}(0^+) = 0 \qquad i=1,2,...,n$$

Then, if $P_{L\Delta}$ is constant for all t, the acceleration in pu is,

$$\frac{1}{\omega_R}\frac{d\omega_{i\Delta}}{dt} = -\frac{P_{sik}}{2H_i}\left(P_{L\Delta}(0^+) \Big/ \sum_{j=1}^{n} P_{sjk} \right) \qquad i=1,2,.....,n \tag{2.74}$$

From the equation (2.74) we can say that the generator rotor decelerates for a positive $P_{L\Delta}$. The pu deceleration of machine *i* is dependent on the synchronizing power coefficient P_{sik} and inertia H_i as per equation (2.74). This deceleration will remain constant until the governor action begins. So after the initial impact the various synchronous machines will be retarded at different rates, each according to its size and its electrical location given by P_{sik}.

2.4.3 Average behavior prior to governor action

Let us analyze the system behavior prior to governor action at time t_1, where t_1 is $0<t_1<t_g$, where t_g =the time when governor action starts.

To obtain the mean deceleration let us define an inertial center that has angle $\bar{\delta}$ and angular velocity $\bar{\omega}$, where by definition,

$$\bar{\delta} \overset{\Delta}{=} \left(1 \Big/ \sum H_i \right) \sum \delta_i H_i \tag{2.75}$$

$$\bar{\omega} \overset{\Delta}{=} \left(1 \Big/ \sum H_i \right) \sum \omega_i H_i \tag{2.75}$$

Summing the set (2.74) for all values of *i*, it is found that

$$\frac{2}{\omega_R} \sum \frac{d}{dt}\left(H_i \omega_{i\Delta}\right) = P_{k\Delta} = -P_{L\Delta}(0^+) \tag{2.77}$$

$$\frac{d}{dt}\frac{\bar{\omega}_\Delta}{\omega_R} = -P_{L\Delta(0^+)} \Big/ \sum_{i=1}^{n} 2H_i \tag{2.78}$$

The equation (2.78) gives the mean acceleration of all the machines in the system, which is defined as the acceleration of a fictitious inertial center.

While the whole system is retarding at the rate given by (2.78) the individual machines are retarding at different rates. Each machine follows an oscillatory motion governed by its swing equation. Synchronizing forces tend to pull them toward the mean system retardation and after the initial transient decays they will acquire the same retardation as of (2.78).In other words when the transient decays $d\omega_{i\Delta}/dt$ will be the same as $d\overline{\omega_{\Delta}}/dt$ as given by equation (2.16).

Substituting the value of $d\omega_{i\Delta}/dt$ from equation (2.78) in equation (2.73), at $t=t_1>t_0$

$$P_{i\Delta}(t_1)=\left(\frac{H_i}{\sum_{j=1}^{n}H_j}\right)P_{L\Delta}(0^+) \tag{2.79}$$

Thus from the equation (2.79), we can find that at the end of a brief transient the various machines shares the increase in load as a function only of their inertia constant. The time t_1 is chosen large enough so that all the machines will have acquired the mean system retardation. At the same time t_1 is not so large as to allow other effects such as governor action to take place.

So finally a decision can be taken from the equations (2.72) and (2.79) that immediately after the impact $P_{L\Delta}$ the machines share the impact according to their electrical proximity to the point of impact as expressed by the synchronizing power coefficient. After a brief transient period the same machines should share the same impact according to inertia constants.

2.5 Effect of *H* constant and line impedance on frequency response

The single machine infinite bus system represented in Fig. 2.1 is simulated to assess the effect of variation of *H* constant and line impedance on frequency.

2.5.1 Effect of *H* constant

As discussed in section 2.3, generators with smaller value of *H* will have higher frequency of oscillation with smaller settling time while generators with larger value of *H* will have lower

frequency of oscillation with greater settling time. Another important response characteristic is the frequency deviations during the initial periods.

The effect of H constant variations on frequency for a single machine infinite bus system is simulated. The simulation is done with damping coefficient K_D = 10 and for the following values of machine inertia constant

H = 2 (blue), 4 (red), 5(green), 7(black)

Figures 2.4 and 2.5 present the effect of H on machine speed (frequency) and rotor angle respectively.

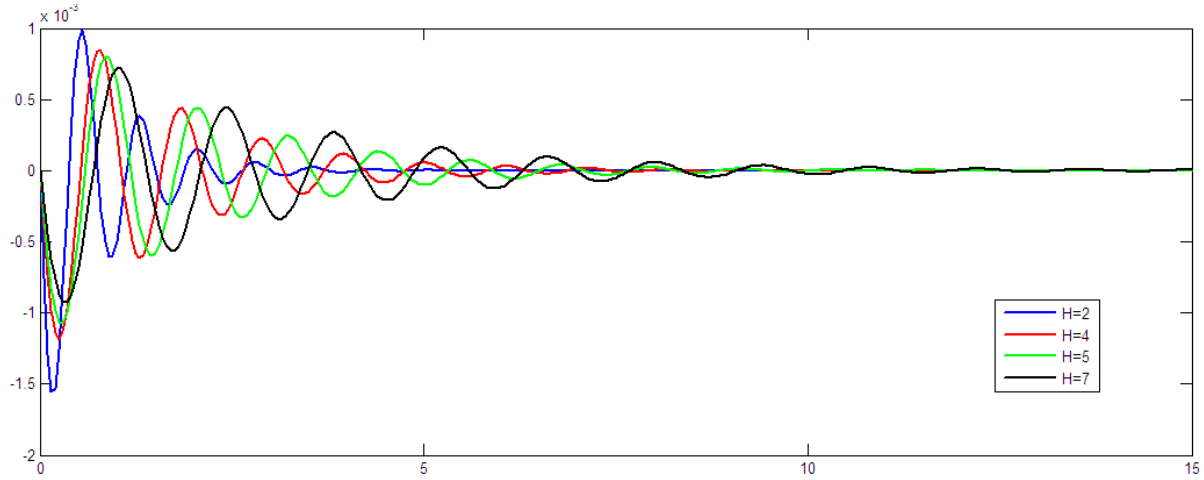

Fig-2.4: Effect of H constant on machine speed (frequency) for a single machine infinite bus system

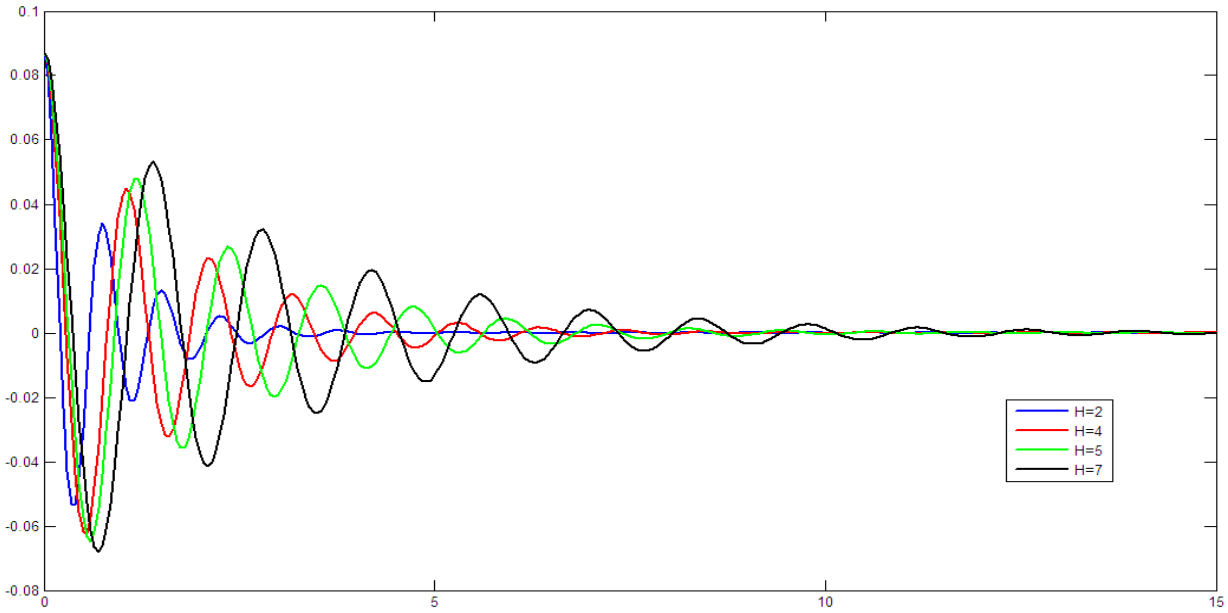

Fig-2.5: Effect of H constant on machine rotor angle for a single machine infinite bus system

From Figs. 2.4 and 2.5 it is seen that machine H constant affects the frequency and angle deviations, the frequency of oscillation and settling time. The frequency deviation is larger for smaller values of H with higher frequency of oscillation. But the settling time is smaller.

2.5.2 Effect of line impedance

The synchronizing torque coefficient K_S directly affects the machine natural frequency and the damping ratio as can be seen from equations (2.58) and (2.59). Increase in K_S increases ω_n and decreases ζ. Since from equation (2.57) K_S is inversely proportional to line impedance, increase in impedance will result is decrease in ω_n and increase in ζ.

The effect of line impedance on frequency for a single machine infinite bus system is simulated. The simulation is done with damping coefficient $K_D = 10$, machine inertia constant H = 3.5 and for the following values of line distance in Km

line distance = 1 (blue), 5 (red), 8 (green), 15 (black)

Figures 2.6 and 2.7 present the effect of line impedance i.e. line distance on machine speed (frequency) and rotor angle respectively.

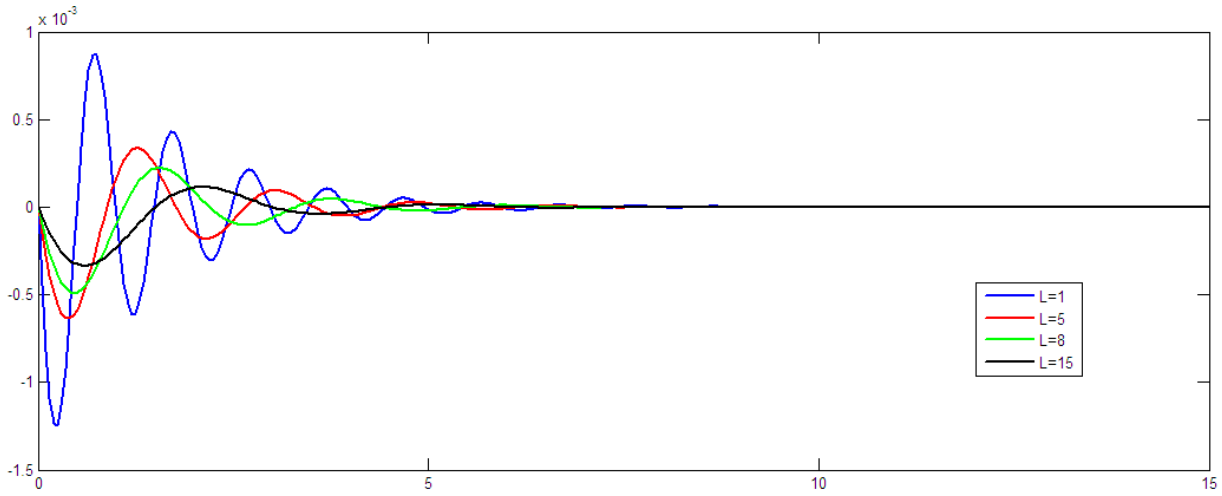

Fig-2.6: Effect of line impedance on machine speed (frequency) for a single machine infinite bus system

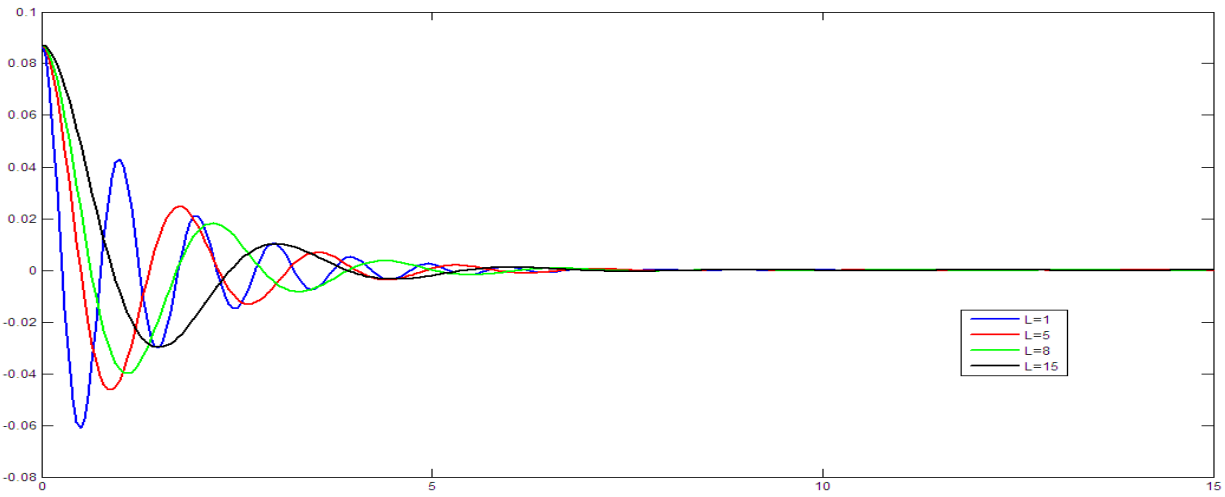

Fig-2.7: Effect of line impedance on machine rotor angle for a single machine infinite bus system

From Figs. 2.6 and 2.7 it is seen that line impedance affects the frequency and angle deviations, the frequency of oscillation. The frequency deviation is larger for smaller values of line impedance with higher frequency of oscillation. Machine rotor angle deviation is also larger for smaller values of line impedance. Effect on settling time is not pronounced.

CHAPTER 3

PREFERENTIAL LOAD SHEDDING METHODOLOGY

3.1 Introduction

It is described in Chapter 2 that initially the impact of load change will be shared immediately by the generators according to their synchronizing power coefficients with respect to the bus at which the load change occurs. Thus, the machines electrically close to the point of impact will pick up the greater share of the load change regardless of their size. After a while the imbalance will be shared according to the generator *H* constant.

Furthermore, it is expected that a load bus with greater amount of load can affect more in terms of frequency change than that with smaller amount of load.

Based on the above analysis, a shedding index is proposed for each load bus depending on the electrical proximity to a generator, the generator *H* constant and the magnitude of load on a bus. No frequency sensitivity analysis is required for calculation of the shedding index. The shedding-index shall help to prepare a priority list for shedding loads in a power system to achieve faster frequency stability under a fault condition.

The proposed strategy of preferential load shedding will reduce the active power absorbed by the loads and make the system frequency restoration faster. The performance of the proposed technique will be verified on a test network by a simulation tool named CYMEPSAF.

3.2 Calculation of the shedding index

Different loads are categorized based on the theory described in Chapter 2. The categorization is done by introducing indexes considering all the components that affect the frequency response of the power system network after a disturbance.

3.2.1 Load bus indexing depending on electrical proximity to generator

In Chapter 2, equation (2.72) shows that a load impact at a network bus is immediately shared by the synchronous generators according to their synchronizing power coefficients. Since synchronizing power coefficient is inversely proportional to electrical distance between load and generator, this distance being proportional to transmission reactance, the response of a

generator electrically closer to the point of a load change impact is faster and greater than that of a generator located farther away. Based on this, a load bus proximity index (*IP*) is proposed.

The *IP* is an integer number and each load bus shall have as many *IP* as there are generators. Let us consider a power system having *n* no. of generators and *m* no. of loads connected to *m* no. of load buses. Let the electrical distance of load bus L_j from the generator G_i be d_{ji}.

where,

$i=1,2,.....,n$ - generator index

$j=1,2,.....m$ - load index

Accordingly, the electrical distances of load bus L_1 from generators $G_1,G_2,.....G_n$ are $d_{11},d_{12},.....d_{1n}$ respectively and the distances of load bus L_m from the generators $G_1,G_2,.....G_n$ are $d_{m1},d_{m2},.....d_{mn}$ respectively. Electrical distances between load and generator is determined by the values of series impedance between the two buses. Table 3.1 presents the proximity index table for the load buses.

Table 3.1: Load indexing based on electrical proximity for an *n* generator and *m* load bus system

Generator	**Proximity Index for load bus**					
	L_1	L_2	.	.	.	L_m
G_1	IP_{11}	IP_{21}	.	.	.	IP_{m1}
G_2	IP_{12}	IP_{22}	.	.	.	IP_{m2}
G_3	IP_{13}	IP_{23}	.	.	.	IP_{m3}
.	.	.	.	.	.	.
.	.	.	.	.	.	.
.	.	.	.	.	.	.
G_n	IP_{1n}	IP_{2n}	.	.	.	IP_{mn}

Let us consider a two generator and two load bus system as shown in Fig. 3.1. The electrical distances, d_{ij}, are such that $d_{11} < d_{12} < d_{21} < d_{22}$. Then the *IP* values shall be as follows:

$IP_{11} > IP_{12} > IP_{21} > IP_{22}$

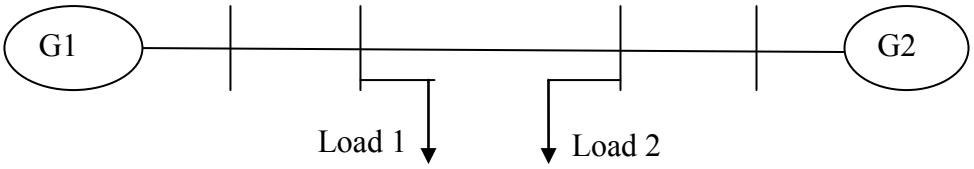

Fig. 3.1: A two generator, two load bus system

Table 3.2 shows the *IP* table for the system shown in Fig. 3.1. As indicated in the table, the value of IP_{11} is 4. It indicates that a change in load on *load bus 1* will invoke the greatest and fastest response from generator *G1*. Thus the *IP* values do not quantify the how much and how fast the response will be, but only the relative amount of response.

Table 3.2: Proximity index (*IP*) for the two generator system

Generator	**Proximity index (*IP*)**	
	Load *L1*	**Load *L2***
G1	4	2
G2	3	1

3.2.2 Generator indexing based on inertia constant

In Chapter 2 it has been described that after a brief transient the impacts of load change in a power system are shared by the generator according to their inertia constant. The generator with higher inertia constant will share greater impact of load change than that of a generator with a lower inertia constant. Equation (2.79) summarizes this. Based on this a generator inertia index (*IH*) is proposed. A generator with a higher inertia constant will have a higher *IH* value.

Let us consider a network having n no. of generators $G_1,G_2.....G_n$ that have inertia constants $H_1,H_2.....H_n$ respectively. Assuming $H_1>H_2> .....>H_n$ the *IH* values will be as follows:

$$IH_1 > IH_2 > ..... > IH_n$$

Table 3.3 presents the *IH* values for the system shown in Fig. 3.1. As indicated in the table, the value of IH_1 is 2 because G_1 has the higher value of inertia constant than that of G_2. It indicates that G_1 will share greater impact of load change than that of G_2. Thus the *IH* values do not quantify the how much and how fast the response will be, but only the relative amount of response.

Table 3.3: Inertia index (*IH*) for the two generator system

Generator	Inertia constant, *H*	Inertia index (*IH*)
G1	5	2
G2	3	1

The summation of the values of inertia indexes for a system is defined as,

$$H_T = \sum_{i=1}^{n} IH_i \tag{3.1}$$

In the case where two or more generators have the same inertia constant they will share the same *IH* value.

3.2.3 Load indexing depending on load size

It is obvious that the size of the load to be shed in an emergency situation is also important to stabilize the power system network quickly. Considering the importance of load size in this respect, loads are also ranked based on its magnitude. The load size index (*IS*) for load *j* is expressed as the ratio of the load connected to a bus to total load of the system,

$$IS_j = \frac{D_j}{\sum_{i=1}^{m} D_i} \tag{3.2}$$

Table 3.5 contains the load data and the load size index (*IS*) for the two generator system shown in Fig: 3.1.

Table 3.4: Load size index for the two generator system

Loads	Load size (MW)	Load size index (*IS*)
L1	20	0.4
L2	30	0.6

3.3 Comprehensive load shedding index

The load bus-generator proximity index (*IP*), generator inertia index (*IH*) and the load size index (*IS*) are combined to form a comprehensive load shedding index (*IL*) for all the loads.

To combine the electrical proximity of the loads to the generator and the effect of generator inertia constant, the proximity-inertia index (*IPH*) is defined as follows

$$IPH_j = \frac{\sum_{i=1}^{n} IP_{ji}.IH_i}{MP} \tag{3.3}$$

where *MP* stands for *maximum point* defined as

$$MP = H_T \text{ x } IP_{max} \tag{3.4}$$

MP is introduced to obtain a normalized value for the proximity-inertia index (*IPH*).

The comprehensive load shedding index (*IL*) for load *j* is now defined as,

$$IL_j = IPH_j + IS_j \tag{3.5}$$

The load with the highest shedding index (*IL*) will have the highest ranking while shedding loads and the load with the lowest value of shedding index will have the lowest ranking. Ranking of loads are done in ascending order according to the *IL* values they obtained i.e. load with the minimum *IL* value is ranked 1 and so on.

Table 3.5 presents the calculated values of the comprehensive load shedding indices (*IL*) for the two generator system shown in Fig 3.1.

Table 3.5: Comprehensive load shedding index (*IL*) for the two generator system

Loads	Proximity-inertia index (*IPH*)	Load size index (*IS*)	Shedding index (*IL*)	Rank
L1	0.92	0.4	1.32	2
L2	0.42	0.6	1.02	1

From Table 3.5 it is found that $IL_1 > IL_2$. So loads on bus *L1* has higher priority to be shed than that of loads on bus *L2* under a falling frequency condition. It is expected that system frequency would respond faster and greater for a change in load on bus *L1* than that on bus *L2*.

CHAPTER 4

TEST SYSTEM AND SIMULATION RESULT

4.1 Introduction

The proposed methodology described in Chapter 3 has been applied to a test network by a simulation tool named CYMEPSAF, which is a new, easier way to handle studies, networks and equipment databases. The technique described in Chapter 3 has been applied to the nine bus test system and the results using the proposed methodology are used in the simulation. The detail of the system has been described in this chapter.

4.2 Nine Bus Test System

A nine bus test system has been developed here to test the proposed methodology. Figure A-1 in Annexure A shows the test system. The test system includes nine buses, four generators, three transformers, six transmission lines and five loads. The loads are connected to buses 2, 3, 5, 6, and 8. The generators are connected to buses 1, 2, 7 and 8. The size of the generators varies from a minimum of 14.56 MW to a maximum of 50 MW. Table A-1 and Table A-2 in Appendix A give the generator data and branch data for the system respectively.

4.3 Preferential load selection from the test system

The technique developed in Chapter 3 has been applied to the nine bus test system and the shedding index for the loads of the test system are calculated.

Table 4.1 shows the electrical distances between generators and loads for the test system.

Table 4.1 Distances between generators and loads in km

Generator	**Loads**				
	L2	***L3***	***L5***	***L6***	***L8***
G1	12	18	5	5	14
G2	0	6	7	7	16
G3	18	12	25	25	34
G4	16	22	9	9	0

The proximity indices (*IP*) for the loads are determined according to Table 4.1, where the lowest value of distance of a load from a generator receives the highest point and vice versa.

In the case where the distance of different loads with respect to different generators is of same value, the loads share the same *IP* value. Table 4.2 presents the *IP* values for the test system.

Table 4.2: Load indexing based on electrical proximity

Generator	Proximity index (*IP*)				
	L2	***L3***	***L5***	***L6***	***L8***
G1	7	4	11	11	6
G2	12	10	9	9	5
G3	4	7	2	2	1
G4	5	3	8	8	12

From Table 4.3, the maximum value of proximity index for the test system

$$IP_{max} = 12$$

Table 4.3 gives the generator inertia constant and inertia index (*IH*) values for the nine bus test system.

Table 4.3: Generator inertia constant and inertia index for the test system

Generator	Inertia constant (*H*)	Inertia index (*IH*)
G1	4	3
G2	3	2
G3	2	1
G4	7	4

Using equation (3.1), the summation of the inertia indices of system

$$H_T = 3+2+1+4 = 10$$

Table 4.5 presents the load magnitude in MW in each load bus and the calculated value of the load size index according to equation (3.2).

Table 4.4: Load data

Load	Load size (MW)	Load size index (*IS*)
L2	25	0.1923
L3	20	0.1538
L5	15	0.1154
L6	40	0.3077
L8	30	0.2307

To calculate the proximity inertia index (*IPH*) using equations (3.3) and (3.4) the first step is to multiply the values of *IP* and *IH* and calculate its total for each load. Using the values of *IP* and *IH* from Tables 4.2 and 4.3 respectively, the calculation is presented in Table 4.5.

Table 4.5: Calculation of *IP* x *IH* for the test system loads

Generator	*IP* x *IH*				
	L2	**L3**	**L5**	**L6**	**L8**
G1	21	12	33	33	18
G2	24	20	18	18	10
G3	4	7	2	2	1
G4	20	12	32	32	48
$\sum IP$ x IH	69	51	85	85	77

Since,

$$IP_{max} = 12$$

$$H_T = 10$$

so, using equation (3.4), maximum point

$$MP = 12 \times 10 = 120$$

Using equation (3.3), proximity-inertia indices for the test system loads are now calculated and presented in Table 4.6.

Table 4.6: Proximity-inertia index (*IPH*) for the test system loads

Load	*IPH*
L2	0.5750
L3	0.4250
L5	0.7083
L6	0.7083
L8	0.6417

Using equations (3.3) – (3.5) the comprehensive load shedding index (*IL*) of the loads in the test system is calculated and presented in Table 4.7. Loads are ranked in ascending order according to the load shedding index (*IL*) value they obtained i.e. load *L3* obtained the minimum *IL* value so it is ranked 1 and so on. Since load L6 obtained the highest *IL* value so it is given the highest rank, in this case 5. This ranking indicates that in case of an emergency loads highest ranking load will be preferred for shedding first for the quickest frequency stabilization. Than *L8*, *L5*, *L2* and finally *L3*.

Table 4.7: Comprehensive load shedding index (*IL*) for the test system

Load bus	Proximity-inertia index (*IPH*)	Load size index (*IS*)	Shedding index (*IL*)	Rank
L2	0.5750	0.1923	0.767307692	2
L3	0.4250	0.1538	0.578846154	1
L5	0.7083	0.1154	0.823717949	3
L6	0.7083	0.3077	1.016025641	5
L8	0.6417	0.2307	0.872435897	4

4.4 Simulation Result

To test the proposed load shedding index formulation different case scenarios are simulated. In case 1, generator *G1* is tripped at 10^{th} cycle and at 20^{th} cycle equal amount of load is shed at two different load buses and compared the frequency responses at different buses. In this case load is shed at the most preferable bus, *L6* (rank 1), and at the least preferable bus, *L3* (rank 5). The frequency response curves are presented in Figures 4.1 to 4.6.

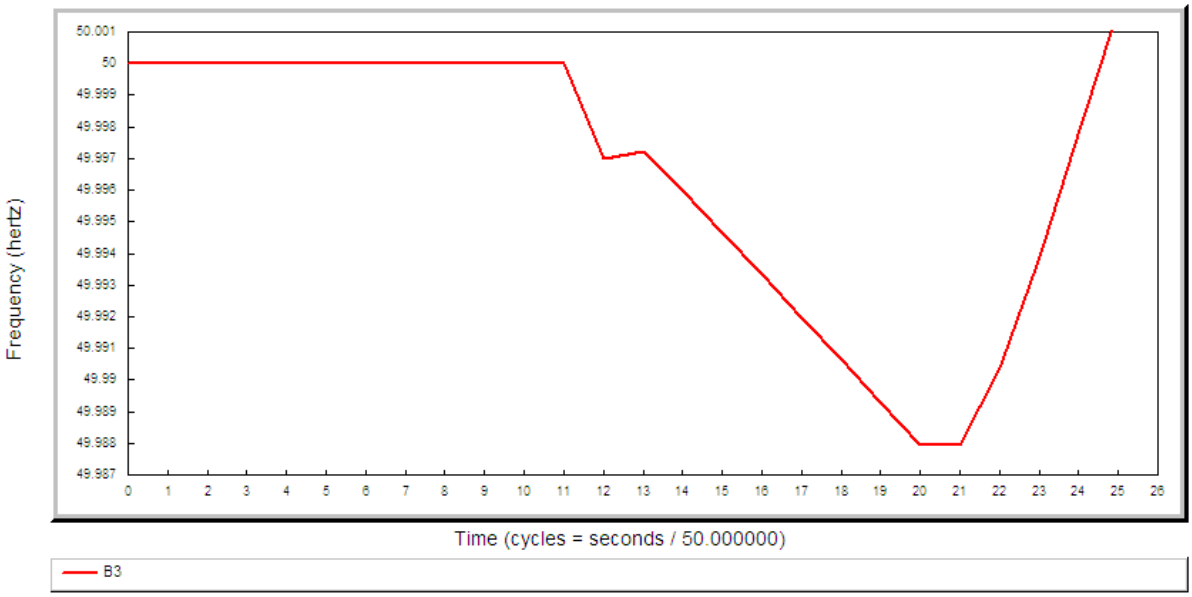

Fig 4.1: Frequency response at bus 3 for load shed at *L6*

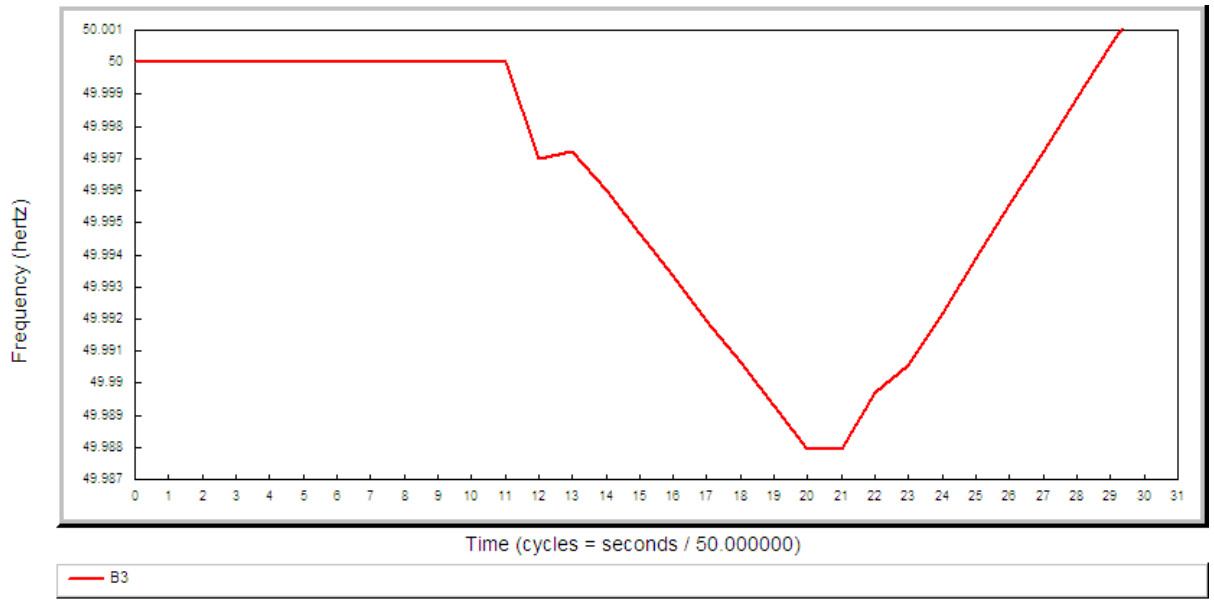

Fig 4.2: Frequency response at bus 3 for load shed at *L3*

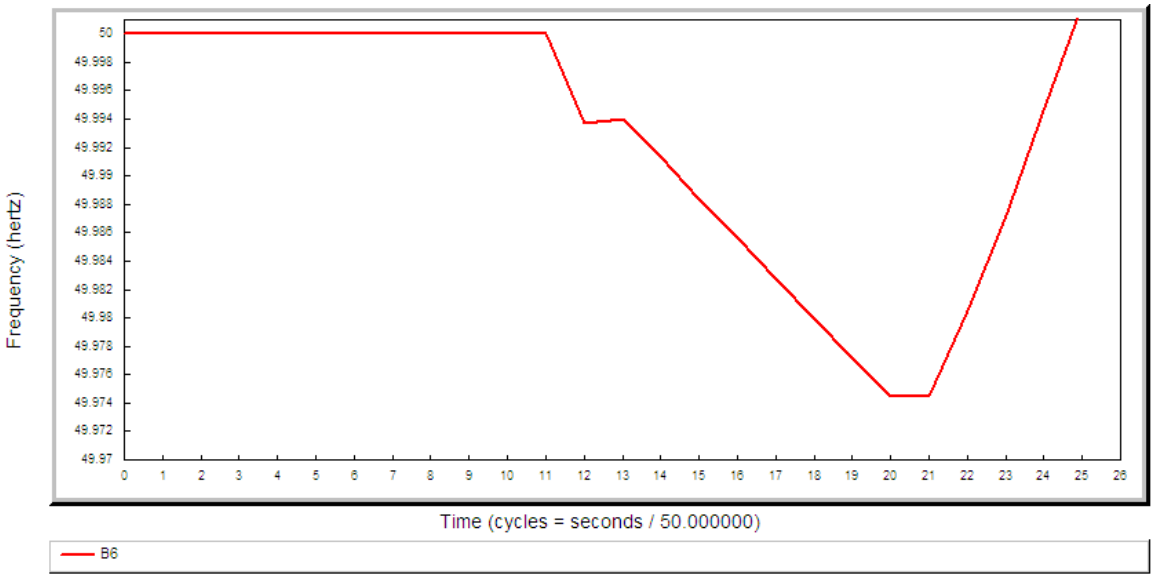

Fig 4.3: Frequency response at bus 6 for load shed at *L6*

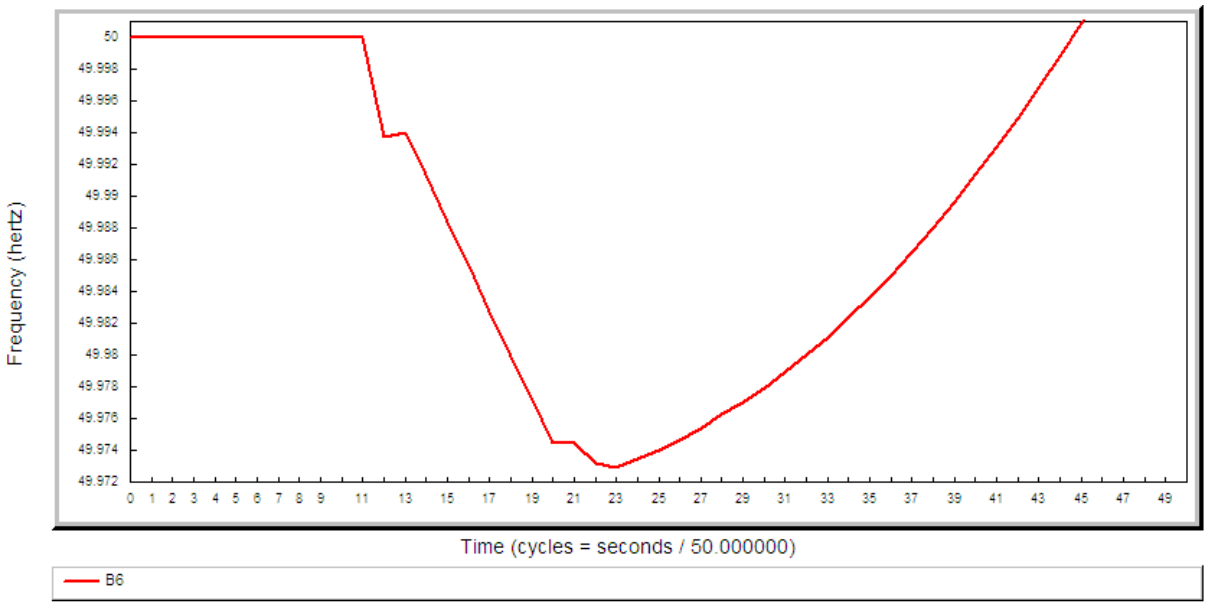

Fig 4.4: Frequency response at bus 6 for load shed at *L3*

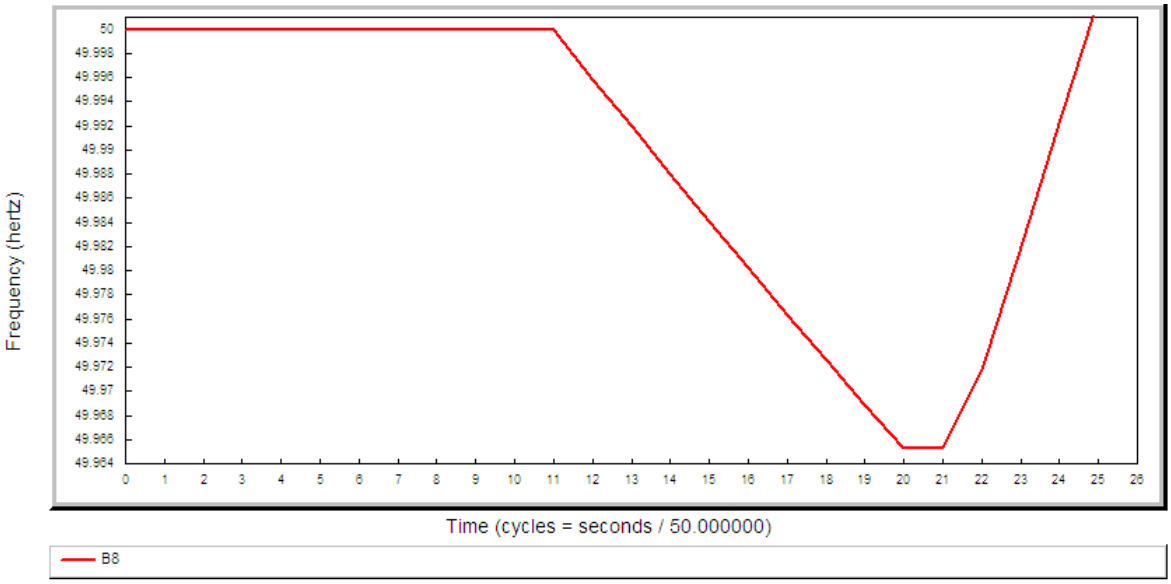

Fig 4.5: Frequency response at bus 8 for load shed at *L6*

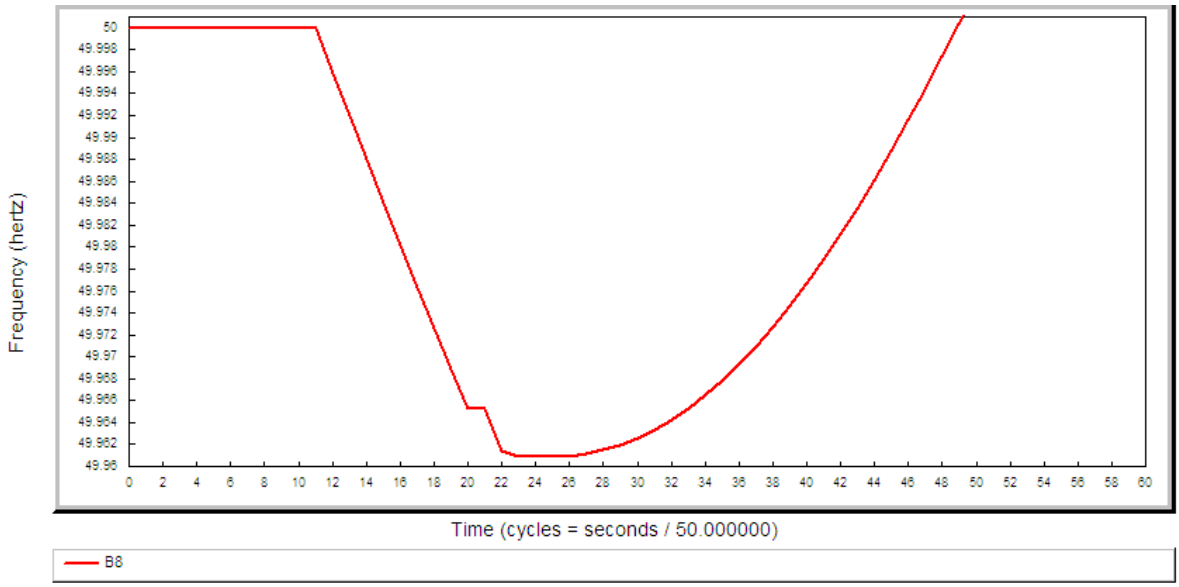

Fig 4.6: Frequency response at bus 8 for load shed at *L3*

The performance is compared by calculating and comparing the slope (m) at the first upward swing of the frequency and the time taken to reach the targeted frequency of 50 Hz. Table 4.7 presents the frequency slopes and Table 4.8 presents the time taken to reach 50 Hz.

Table 4.8 Comparison of frequency slope (*m*) for case 1

Frequency monitored at bus	Slope *m* in Hz/sec for load shed at bus		Comparison of slope
	L6	***L3***	
Bus 2	-0.00025	0	*m3 > m6*
Bus 3	0.000375	0.0008	*m6 > m3*
Bus 5	0.001285714	0.000125	*m6 > m3*
Bus 6	0.001333333	0.000111111	*m6 > m3*
Bus 8	0.002	-0.000375	*m6 > m3*

Table 4.9 Comparison of time taken to reach 50 Hz for case 1

Frequency monitored at bus	Time taken in sec to reach 50 Hz for load shed at bus	
	L6	***L3***
Bus 2	83	77
Bus 3	56	37
Bus 5	42	56
Bus 6	42	55
Bus 8	41	57

Table 4.8 shows that the frequency of most of the buses rises more sharply for the most preferable load (*L6*) than that for the least preferable load (*L3*). Table 4.9 shows that the time taken to reach the 50 Hz is lower for the most preferable load bus (*L6*) than that for least preferable load bus (*L3*). In case of buses 2 and 3 the time taken to reach 50 Hz is smaller for load shed at *L3* than that for load shed at *L6*. The reason for this is bus 2 is electrically nearer to *L3* than *L6* and bus 3 is the bus where load *L3* is connected.

In case 2, generator *G2* (30 MW) is tripped at 10^{th} cycle and at 20^{th} cycle load is shed. Similarly, in case 3 generator *G3* (50 MW) is tripped and in case 4 generator *G4* (40 MW) is tripped.

Tables 4.10, 4.11 and 4.12 presents the performance comparison in terms of frequency slope for load shed at the most preferable load (*L6*) and at the least preferable load (*L3*) for all three cases.

Table 4.10 Comparison of frequency slope (*m*) for case 2

Frequency monitored at bus	Slope *m* in Hz/sec for load shed at bus		Comparison of slope (*m*)
	L6	***L3***	
Bus 2	0.004015	0.0005	*m6 > m3*
Bus 3	0.003	0.001333	*m6 > m3*
Bus 5	0.005	0.000833	*m6 > m3*
Bus 6	0.005	0.000833	*m6 > m3*
Bus 8	0.004	-0.0012	*m6 > m3*

Table 4.11 Comparison of frequency slope for case 3

Frequency monitored at bus	Slope *m* in Hz/sec for load shed at bus		Comparison of slope (*m*)
	L6	***L3***	
Bus 2	-0.00225	-0.00267	*m6 > m3*
Bus 3	-0.001	-0.003	*m6 > m3*
Bus 5	-0.0008	-0.00433	*m6 > m3*
Bus 6	-0.00075	-0.005	*m6 > m3*
Bus 8	-0.002	-0.00733	*m6 > m3*

Table 4.12 Comparison of frequency slope for case 4

Frequency monitored at bus	Slope *m* in Hz/sec for load shed at bus		Comparison of slope (*m*)
	L6	***L3***	
Bus 2	-0.00086	-0.00114	*m6 > m3*
Bus 3	0.000385	-0.00209	*m6 > m3*
Bus 5	0.002667	0.0136	*m6 > m3*
Bus 6	0.003	-0.00343	*m6 > m3*
Bus 8	0.00275	-0.004	*m6 > m3*

From Table 4.10, Table 4.11 and Table 4.12 it is observed that the frequency of the load buses rises more sharply for the most preferable load (*L6*) shed than that of for the least preferable load (*L3*) shed.

Table 4.13 shows the comparison between time taken to reach 50 Hz frequency for preferable load (*L6*) shed and that for the least preferable load (*L3*) shed for case 2.

Table 4.13 Comparison of time taken to reach 50 Hz for case 2

Frequency monitored at bus	**Time taken in sec to reach 50 Hz for load shed at bus**	
	L6	***L3***
Bus 2	24.5	33.0
Bus 3	25.0	29.3
Bus 5	24.0	40.0
Bus 6	24.0	40.0
Bus 8	23.4	51.0

From Table 4.13 it is seen that the time taken for the frequency to reach the 50 Hz is lower for the most preferable load (*L6*) shed than that for the least preferable load (*L3*) shed.

For case 3, generator *G3* tripping, the frequency of the system cannot reach up to 50 Hz for both the cases as the capacity of the G3 is higher than both the loads (*L6* and *L3*).

For case 4, generator *G4* tripping, the frequency of the system cannot reach up to 50 Hz for the case of the least preferable load (*L3*) shed.

So finally from the above analysis, it can be said that the system frequency tries to settle more quickly for the case of the most preferable load shed than that of for any other less preferable load shed. We may conclude that the application of the proposed preferential load shedding technique on a nine bus test system and the simulation result validate the proposed technique.

CHAPTER 5

CONCLUSION

5.1 Conclusion

Load shedding is an important tool to save power network. An intelligent load shedding technique can protect the network more quickly. Presently load shedding is done by measuring frequency and voltage changes, rate of change of frequency, load frequency regulation factor etc. These studies need online measurement.

In a power system network, the response of a generator closer to the point of disturbance that creates the imbalance between the load and generation is faster than that of a generator located at a far distant location with respect to the disturbance. At the moment of any disturbance that creates the imbalance between the load and generation, imbalance between the system load and generation is distributed among the generators according to their electrical distance with the load change location. As the load imbalance distribution changes with time, the imbalance is distributed according to the inertias of generators.

Thus, the machines electrically close to the point of impact pick up the greater share of the load change regardless of their size. After a while the imbalance is shared according to the generator *H* constant.

Furthermore, loads can be treated as a resource that can be used to stabilize system frequency by shedding. Hence the larger the load size the greater its potential towards contributing frequency stabilization.

Based on the above analysis, in this work loads to be shed are prioritized off line based on the power system network data. A shedding-index is calculated for each load depending on the electrical proximity of the loads to generators, the generator inertia constant (*H)* and the size of the load. The shedding-index helps to prepare a priority list for shedding loads in a power system to achieve faster frequency stability under a fault condition.

The performance of the proposed technique is verified on a nine bus test network. Simulations verified the method of preferential load shedding technique based on the calculated load shedding index.

5.2 Further works

The technique developed in this work can be explored in the following areas:

1. Extending the technique to include successive load shedding.
2. Incorporating online measurement data for selecting the load to be shed.
3. Stability analysis of the proposed technique.

REFERENCES

[1] Dadashzadeh, M. R., Pasand, M. Sanaye, "Simulation and Investigation of Load Shedding algorithms for a real network using dynamic modeling''

[2] Delfino, B., Massucco, S., Morini A., Scalera, P. , Silvestro, F., "Implementation and comparison of different under frequency load-shedding schemes", *IEEE Power Engineering Society Summer Meeting*, Vol. 1, pp. 307– 312, 15-19 July 2001

[3] Walter, A, Protective Relaying Theory and Applications, Ed. Elmore: Marcel Dekker Inc., 1994

[4] Kundur, P., Power system stability and control, McGraw Hill, 1994

[5] Anderson, P. M., Mirheydar, M., "An adaptive method for setting underfrequesncy load shedding relay," *IEEE Transaction on Power Systems*, Vol. 7, No. 2, May 1992

[6] Anderson, P.M., "Power system protection", IEEE Press 1999, pp. 807-851

[7] You, Haibo, Vittal, Vijay, Yang, Zhong, "Self-healing in power systems: an approach using islanding and rate of frequency decline-based load shedding", *IEEE Transactions of Power Systems,* Vol. 18, No. 1, pp. 174-181, February 2003

[8] Ahmed, S. Shahnawaz*,* Sarker, Narayan C.*,* Khairuddin, Azhar B, Ghani, Mohd Ruddin B Abd, Ahmad, Hussein, "A Scheme for Controlled Islanding to Prevent Subsequent Blackout", *IEEE Transactions on Power Systems,* Vol. 18, No. 1, pp. 136-143, February 2003

[9] Prastijio, D., Lachs, W. R. and Sutants, D., "A New Load Shedding Scheme for Limiting Under Frequency", *IEEE Transaction on Power Systems*, Vol. 9, No. 3, pp. 1371-1377, August 1994

[10] You, H., Vittal, V., and Wang, X., "Slow coherency-based islanding," *IEEE Transaction on Power Systems*, Vol. 19, No. 1, pp. 483–491, February 2004

[11] Jung, Juhwan*,* Liu, Chen-Ching*,* Tanimoto, Steven L. *and* Vittal, Vijay*,* "Adaptation in load shedding under vulnerable operating conditions," *IEEE Transaction on Power Systems*, Vol. 17, No. 4, November 2002

[12] Terzija, Vladimir V.*,* "Adaptive under frequency load shedding," *IEEE Transaction on Power Systems*, Vol. 21, No. 3, August 2006

[13] Concordia, Charles, Fink, Lester H., Poullikkas, George "Load shedding on an isolated system," *IEEE Transaction on Power Systems*, Vol. 10, No. 3, August 1995

[14] Xiong, Xiaofu and Li, Wenyuan, "New under frequency load-shedding scheme considering load frequency characteristics," International Conference on Power System Technology, 2006

[15] Parniani, M. and Nasri, A. "SCADA based underfrequency load-shedding integrated with rate of frequency decline", IEEE Power Engineering Society General Meeting, 2006

[16] Prastijio, D., Lachs, W. R. and Sutants, D., "A New Load Shedding Scheme for Limiting Under Frequency", *IEEE Transaction on Power System*, Vol. 9, No. 3, pp. 1371-1377, August 1994

[17] Ahsan, Q., Chowdhury, A. Hasib, Ahmed, S. Shahnawaz, Bhuyan I. H., Haque, M. A., Rahman, H., "Technique to Develop Auto Load Shedding and Islanding Scheme to Prevent Power System Blackout", *IEEE Transaction on Power Systems*, February 2012

[18] Anderson, P.M. and Fouad A.A., Power system control and stability, Second edition, IEEE Press, 2002

[19] Shokooh, Shervin, Khandelwal, Tanuj, Dr. Shokooh, Farrokh, Tastet, Jacques, Dr. Dai, JJ, "Intelligent Load Shedding Need for a Fast and Optimal Solution", IEEE PCIC Europe 2005

[20] Lu, Ying, Kao, Wen-Shiow, Chen, Yung-Tien , "Study of Applying Load Shedding Scheme With Dynamic D-Factor Values of Various Dynamic Load Models to Taiwan Power System", *IEEE Transaction on Power Systems*, Vol. 20, No. 4, November 2005

[21] Zin, A.A. Mohd, Hafiz, H. Mohd, Aziz, M.S. , "A Review of Under-frequency Load Shedding Scheme on TNB System", National Power & Energy Conference (PECon) 2004 ProcccdinKs, Kuala Luinliirr. Malaysia

[22] Gjukaj, A., Kabashi G., Pula, G., Avdiu, N., Prebreza, B., "Re-Design of Load Shedding Schemes of the Kosovo Power System", *Journal of World Academy of Science, Engineering and Technology* (74), 2011

[23] Cho, Boungwook , Kim, Heechul, Almulla, Musaab M. , Seeley, Nicholas C. , "The Application of a Redundant Load-Shedding System for Islanded Power Plants," Proc. of 5th IEEE GCC Conference & Exhibition, pp, 1-6, March 2009

[24] Seyedi, H., Sanaye-Pasand, M. , "Design of New Load Shedding Special Protection Schemes for a Double Area Power System", *American Journal of Applied Sciences*, Vol 6, No. (2, pp. 317-327, 2009

[25] Thalassinakis, E. J., Dialynas, E. N., and Agoris, D., "Method combining anns and monte carlo simulation for the selection of the load shedding protection strategies in autonomous power systems," *IEEE Transactions on Power Systems*, Vol. 21, No. 4, pp. 1574–1582. 2006

[26] Faranda, R., Pievatolo, A., and Tironi, E., "Load shedding: A new proposal," *IEEE Transactions on Power Systems*, Vol. 22, No. 4, pp. 2086–2093, 2007

[27] Anderson, P.M and Mirheydar, M., "A low-order system frequency response model", *IEEE Transactions on Power Systems*, Vol. 5, No. 3, pp. 720-729, Aug. 1990

APPENDIX A

NINE BUS TEST SYSTEM

The Nine bus test system data is presented in Appendix A. Figure A-1 presents the transmission network of the system. Table A-1 gives the bus data. Table A-2 in gives the branch data for the system. Table A-3 gives the generator data and Table A-4 gives the load data of the test system.

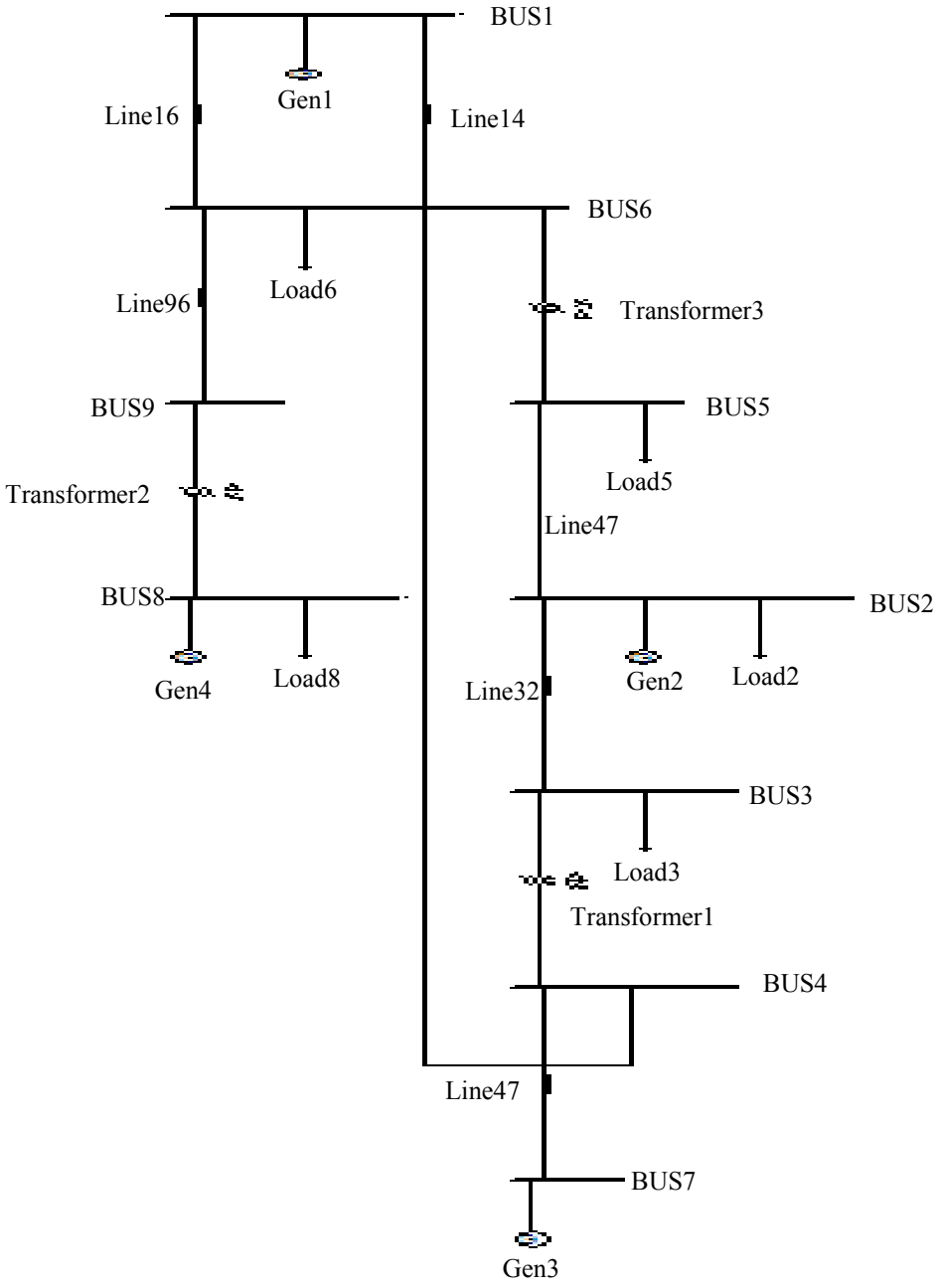

Figure A-1: Nine bus test system

Table A-1: Bus data

Bus ID	Base KV	P Gen (MW)	Q Gen (MW)	P Load (MW)	Q Load (MVAR)
B1	69	14.56	18.03	0	0
B2	13.8	30	10.89	25	10
B3	13.8	0	0	20	6
B4	69	0	0	0	0
B5	13.8	0	0	15	4
B6	69	0	0	40	10
B7	69	50	0.54	0	0
B8	13.8	40	12.6	30	10
B9	69	0	0	0	0

Table A-2: Branch data

BUS From	BUS To	kV nominal	Length (KM)	P (MW)	Q (MVAR)	S (MVA)	Pf (%)
B5	B2	13.8	70	-3.64	0.62	3.69	-98.6
B3	B2	13.8	60	-1.11	-0.4	1.19	-94
B1	B4	69	100	-27.72	9.96	29.46	-94.1
B1	B6	69	50	42.28	8.07	43.04	98.2
B9	B6	69	90	9.99	2.46	10.29	97.1
B4	B7	69	120	-47.45	6.14	47.85	-99.2

Table A-3: Generator data

Gen ID	H	BUS ID	Rated S (MVAR)	KV Nominal	P (MW)	Q (MVAR)	S (MVA)	PF(%)
G1	4	B1	500	69	14.56	18.03	23.17	62.8
G2	3	B2	300	13.8	30	10.89	31.91	94
G3	2	B7	500	69	50	0.54	50	100
G4	7	B8	300	13.8	40	12.6	41.94	95.4

Table A-4: Load data

ID	BUS ID	P (MW)	Q (MVAR)	S (MVA)	Pf (%)
LOAD8	B8	30	10	31.62	94.9
LOAD2	B2	25	10	26.93	92.8
LOAD3	B3	20	6	20.88	95.8
LOAD5	B5	15	4	15.52	96.6
LOAD6	B6	40	10	41.23	97